Available online at www.sciencedirect.com
ScienceDirect
Mechanism and Machine Theory 43 (2008) 310–334
Mechanism and Machine Theory
www.elsevier.com/locate/mechmt

Balancing of shaking forces and shaking moments for planar mechanisms using the equimomental systems

Himanshu Chaudhary *, Subir Kumar Saha

Department of Mechanical Engineering, Indian Institute of Technology Delhi, Hauz Khas, New Delhi 110016, India

Received 30 March 2006; received in revised form 27 March 2007; accepted 6 April 2007
Available online 7 June 2007

Abstract

A general mathematical formulation of optimization problem for balancing of planar mechanisms is presented in this paper. The inertia properties of mechanisms are represented by dynamically equivalent systems, referred as equimomental systems, of point-masses to identify design variables and formulate constraints. A set of three equimomental point-masses for each link is proposed. In order to determine the shaking forces and the shaking moments, the dynamic equations of motion for mechanisms are formulated systematically in the parameters related to the equimomental point-masses. The formulation leads to an optimization scheme for the mass distribution to improve the dynamic performances of mechanisms. The method is illustrated with two examples. Balancing of combined shaking force and shaking moment shows a significant improvement in the dynamic performances compared to that of the original mechanisms.

Keywords: Multiloop mechanism; Optimization; Shaking force; Shaking moment; Equimomental system

1. Introduction

Balancing of shaking forces and shaking moments in mechanisms is important in order to improve their dynamic performances and fatigue life by reducing vibration, noise and wear. Several methods are developed to eliminate the shaking forces and shaking moments in planar mechanisms. The methods to completely eliminate the shaking force are generally based on making the total mass centre of a mechanism stationary. Different techniques are used for tracing and making it stationary. The method of *principal vectors* [1] describes the position of the mass centre by a series of vectors that are directed along the links. These vectors trace the mass centre of the mechanism at hand and the conditions are derived to make the system mass centre stationary. A more referred method in the literature is the method of *linearly independent vectors* [2], which make the total mass centre of a mechanism stationary. This is achieved by redistributing the link masses in such a

* Corresponding author. Tel.: +91 11 26591135; fax: +91 11 26582053.
E-mail addresses: himanshubhl@rediffmail.com (H. Chaudhary), saha@mech.iitd.ernet.in (S.K. Saha).

0094-114X/$ - see front matter © 2007 Elsevier Ltd. All rights reserved.
doi:10.1016/j.mechmachtheory.2007.04.003

manner that the coefficient of the time-dependent terms of the equations describing the total centre of mass trajectory vanish. Kosav [3] presented a general method using ordinary vector algebra instead of the complex number representation of the vectors [2] for full force balance of planar linkages. One of the attractive features of a force-balanced linkage is that the shaking force vanishes, and the shaking moment reduces to a pure torque which is independent of reference point. However, only shaking force balancing is not effective in the balancing of mechanism. There are many drawbacks of the complete shaking force balancing. For example, (a) it mostly increases the total mass of the mechanism, (b) it needs some arrangement like counterweights to add increased mass, and (c) it increases the other dynamic characteristics, e.g., shaking moment, driving torque, and bearing reactions. The influence of the complete shaking force balancing is thoughtfully investigated by Lowen et al. [4] on the bearing reactions, input-torque, and shaking moment for a family of crank-rocker four-bar linkages. This study shows that these dynamic quantities increase and in some cases their values rise up to five-times.

Several authors attempted the balancing problem as a complete shaking force and shaking moment balancing. Elliot and Tesar [5] developed a theory of torque, shaking force, and shaking moment balancing by extending the method of linearly independent vectors. Complete moment balancing is also achieved by a cam-actuated oscillating counterweight [6], inertia counterweight and physical pendulum [7], and geared counterweights [8–10]. More information on complete shaking moment balancing can be obtained in a critical review by Kosav [11], and Arakelian and Smith [12]. Practically these methods not only increase the mass of the system but also increase its complexity.

An alternate way to reduce the shaking force and shaking moment along with other dynamic quantities such as input-torque, bearing reactions, etc., is to optimize all the completing dynamic quantities. Since shaking moment reduces to a pure torque in a force-balanced linkage, many researchers used the fact to develop their theory of shaking moment optimization. Berkof and Lowen [13] proposed an optimization method for the root-mean-square of the shaking moment in a fully force-balanced in-line four-bar linkage whose input link is rotating at a constant speed. As an extension of this method Carson and Stephenes [14] highlighted the need to consider the limits of feasibility of the link parameters. A different approach for the optimization of shaking moment in a force-balanced four-bar linkage is proposed by Hains [15]. Using the principle of the independence of the static balancing properties of a linkage from the axis of rotation of the counterweights, partial shaking moment balancing is suggested in [16]. On the other hand, the principle of momentum conservation is used by Wiederrich and Roth [17] to reduce the shaking moment in a fully force-balanced four-bar linkage.

Dynamic quantities, e.g., shaking force, shaking moment, input-torque, etc., depend on the mass and inertia of each link, and its mass centre location. These inertia properties of mechanism can be represented more conveniently using the dynamically equivalent system of point-masses [18,21]. The dynamically equivalent system is also referred as *equimomental system.* The concept is further elaborated by Wenglarz et al. [19] and Huang [20]. Using the concept of equimomental system Sherwood and Hockey [21] presented the optimization of mass distribution in mechanisms. Hockey [22] discussed the input-torque fluctuations of mechanisms subject to external loads by means of properly distributing the link masses. Using the two point-mass model, momentum balancing of four-bar linkages was presented in [17]. Optimum balancing of combined shaking force, shaking moment, and torque fluctuations in high speed linkages is reported in [23,28], where a two point-mass model was used. The concept can also be applied for kinematic and dynamic analyses of mechanisms [24,25], and the minimization of inertia-induced forces [26,27] of spatial mechanisms. Although scattered, the applications of equimomental system are found in the above literatures. None of them, however, presents a comprehensive study of the concept and its application in the balancing of mechanisms.

As discussed above, only shaking force balancing of mechanisms does not imply their balancing of shaking moment. In order to reduce inertia-induced forces, e.g., the shaking force and shaking moment, along with other dynamic quantities such as input-torque and bearing reactions, it is required to trade-off among these competing dynamic quantities. The analytical solution to the optimization of shaking force and shaking moment is difficult, and possible only for simple planar linkages. Hence, balancing aspect of mechanisms is postulated as an optimization problem in this paper. Once the mathematical optimization problem is formulated, one can use the existing computer libraries to solve it. The formulation of the optimization problem, nevertheless, is difficult because it needs the following:

1. formulation of dynamic equations to calculate the joint reactions and other dynamic characteristics;
2. identification of the design variables and formulation of the constraints that define the design space of feasible solutions; and
3. an objective function which is to be used as an index of merit for the dynamic performance of a linkage at hand.

In this paper, the first difficulty is overcome by formulating the equations of motion of a closed-loop system in minimal set using the joint-cut method. Concerning the second difficulty, the design variables and the constraints are identified by introducing the equimomental system of point-masses. The formulation leads to an optimization scheme for the mass distribution of bodies to optimize the dynamic performances, e.g., shaking force and shaking moment, and driving torque fluctuations. A novelty of the present approach is that the balancing problem of mechanisms is formulated as a general mathematical optimization problem. The methodology is quite general and not restricted only to single-loop four-bar linkage as reported in [28]. The dynamic analysis presented in [28] is extended in this paper for multiloop systems as well. The optimization methodology proposed in this paper is also more effective than those reported in [23,28], as explained in Section 4.1.2. It gives flexibility to the designer to put constraints according to the application. Our original claims in this paper are: (i) the dynamic modelling of an n-link multiloop mechanism, (ii) the formulation of the optimization problem for the n-link multiloop mechanism, and (iii) the use of three point-mass systems for the dynamic modelling and optimization of the mechanism mentioned in steps (i) and (ii) above. The proposed methodology is illustrated with two examples. In the first example, a four-bar linkage is considered. The effectiveness of the method is shown by comparing the analytical results [2] for full force balancing of the four-bar linkage. The other example is multiloop mechanism used in carpet scraping machine for cleaning carpets.

This paper is organized as follows. Section 2 explains the concept of equimomental system for a rigid body undergoing in a plane motion. Optimization problem formulation for a mechanism using the equimomental concept is shown in Section 3. The effectiveness of the methodology is illustrated in Section 4 using two mechanisms. Finally, conclusions are given in Section 5. Two Appendices A and B are provided additionally to derive the equations of motion using three point-mass model and its comparison with two point-mass model, respectively.

2. Equimomental system

A comprehensive study of the equimomental system of a rigid body undergoing in a plane motion is presented in this section. The sets of equimomental point-masses for the rigid body are proposed in order to obtain equimomental system of the original system consisting of interconnected rigid bodies. The concept is illustrated using three point-mass model.

As shown in Fig. 1, consider a rigid body whose the centre of mass at C and a coordinate frame OXY fixed to it at O. Motion of the body takes place in the XY plane. We seek a set of dynamically equivalent system of n

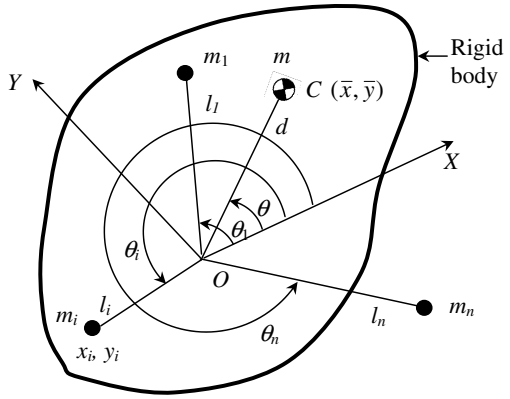

Fig. 1. Dynamic equivalence of a planar rigid body.

point-masses rigidly fixed to the local frame. Each point-mass has its mass m_i and located at coordinates (x_i, y_i) in the local frame. For planar motion, the requirements of the dynamical equivalence of the system of point-masses and the original rigid body are [19]: (a) the same mass; (b) the same centre of mass; and (c) the same moment of inertia about an axis perpendicular to the plane and passing through origin, O, i.e.,

$$\sum_{i=1}^{n} m_i = m \tag{1}$$

$$\sum_{i=1}^{n} m_i x_i = m\bar{x}; \quad \sum_{i=1}^{n} m_i y_i = m\bar{y} \tag{2)–(3}$$

$$\sum_{i=1}^{n} m_i (x_i^2 + y_i^2) = I_c + m(\bar{x}^2 + \bar{y}^2) \tag{4}$$

where m and I_c are the mass and the moment of inertia about the centre of mass, $C(\bar{x}, \bar{y})$, of the rigid body, respectively.

Since each mass introduces three parameters (m_i, x_i, y_i) to identify it, $3n$ parameters are required for n point-masses. Only four parameters out of them can be obtained uniquely from Eqs. (1)–(4) assigning the remaining $(3n - 4)$ arbitrary values. The number of arbitrarily assigned parameters increases with the number of point-masses. With a single point-mass having only three unknown parameters and four equations, Eqs. (1)–(4), lead to overdetermined system of equations, which has no solution unless the equations are consistent. Moreover, two point masses have the six unknown parameters [28]. The four parameters out of them can be solved uniquely assigning the other two. Hence, minimum two point masses are required to represent a rigid body moving in a plane. However, it is not always possible to get all point-masses positive.

To illustrate the procedure of finding a set of dynamically equivalent point-masses, consider a three point-mass model of a rigid body moving in the XY plane. The polar coordinates, Fig. 1, of the point-masses are (l_i, θ_i), for $i = 1, 2, 3$, where $l_i \equiv \sqrt{x_i^2 + y_i^2}$ and $\theta_i \equiv \tan^{-1}(y_i/x_i)$. The three point-mass model would then be dynamically equivalent to the original rigid body if Eqs. (1)–(4) are satisfied, i.e.,

$$\sum_{i=1}^{3} m_i = m \tag{5}$$

$$\sum_{i=1}^{3} m_i l_i C\theta_i = mdC\theta; \quad \sum_{i=1}^{3} m_i l_i S\theta_i = mdS\theta \tag{6)–(7}$$

$$\sum_{i=1}^{3} m_i l_i^2 = mk^2 \tag{8}$$

where $d \equiv \sqrt{\bar{x}^2 + \bar{y}^2}$ and $\theta \equiv \tan^{-1}(\bar{y}/\bar{x})$ are polar coordinates of the mass centre of the rigid body. Moreover, $S\theta \equiv \sin\theta$, $C\theta \equiv \cos\theta$, and $mk^2 \equiv I_c + md^2 - k$ being the radius of gyration about the point, O. Note that there are nine unknowns, namely, m_i, l_i, and θ_i, for $i = 1, 2, 3$, and four equations. Now, it is important to decide which five parameters would be chosen arbitrarily so that the remaining four are solved uniquely. It is advisable to choose l_i and θ_i so that the dynamic equivalence conditions become linear in point-masses. Hence, assigning l_2, l_3 and θ_i, for $i = 1, 2, 3$, the remaining, i.e., four parameters, m_1, m_2, m_3, and l_1 are determined uniquely using Eqs. (5)–(8). Assuming $l_2 = l_1$; $l_3 = l_1$ and substituting them in Eq. (8), yields $l_1 = \pm k$. Taking the positive value for l_1 that is physically possible, the three point-masses are then determined from Eqs. (5)–(7). Substituting $l_1 = k$ in Eqs. (5)–(7), these equations can be written as

$$\mathbf{Km} = \mathbf{b} \tag{9}$$

where the 3×3 matrix, $\mathbf{K}$, and the 3-vectors, $\mathbf{m}$ and $\mathbf{b}$ are as follows:

$$\mathbf{K} \equiv \begin{bmatrix} 1 & 1 & 1 \\ kC\theta_1 & kC\theta_2 & kC\theta_3 \\ kS\theta_1 & kS\theta_2 & kS\theta_3 \end{bmatrix}; \quad \mathbf{m} \equiv \begin{bmatrix} m_1 \\ m_2 \\ m_3 \end{bmatrix}; \quad \mathbf{b} \equiv \begin{bmatrix} m \\ mdC\theta \\ mdS\theta \end{bmatrix} \tag{10}$$

From Eq. (9), it is clear that the solution for $\mathbf{m}$ exists if $\det(\mathbf{K}) \neq 0$, i.e., $\theta_1 \neq \theta_2$, $\theta_1 \neq \theta_3$, and $\theta_2 \neq \theta_3$. It means that any two point masses should not lie on the same radial line emanating from the origin O. The vector $\mathbf{m}$ can be obtained as

$$\mathbf{m} = \mathbf{K}^{-1}\mathbf{b} \tag{11}$$

where $\mathbf{K}^{-1}$ is evaluated as

$$\mathbf{K}^{-1} \equiv \frac{k}{\det(\mathbf{K})}\begin{bmatrix} kS(\theta_3-\theta_2) & (S\theta_2 - S\theta_3) & (C\theta_3 - C\theta_2) \\ -kS(\theta_3-\theta_1) & (S\theta_3 - S\theta_1) & (C\theta_1 - C\theta_3) \\ -kS(\theta_1-\theta_2) & (S\theta_1 - S\theta_2) & (C\theta_2 - C\theta_1) \end{bmatrix} \tag{12}$$

in which, $\det(\mathbf{K}) \equiv k^2[S(\theta_3-\theta_2) + S(\theta_2 - \theta_1) + S(\theta_1-\theta_3)]$. It is evident from the solution, Eq. (11), that the sum of the point-masses is equal to the mass of the body for any values of angles except $\theta_1 \neq \theta_2$, $\theta_1 \neq \theta_3$, and $\theta_1 \neq \theta_3$. Note here that, there is a possibility of some point masses becoming negative. However, it does not hindrance the process of representing the rigid body as long as the total mass and the moment of inertia about the polar axis through centre of mass give positive value [21]. As an example, if $\theta_1 = 0$; $\theta_2 = 2\pi/3$; and $\theta_3 = 4\pi/3$, the point masses are calculated as

$$m_1 = \frac{m}{3}\left(1 + \frac{2}{k}dC\theta\right); \quad m_2 = \frac{m}{3}\left(1 - \frac{dC\theta}{k} + \frac{\sqrt{3}dS\theta}{k}\right); \quad \text{and}$$
$$m_2 = \frac{m}{3}\left(1 - \frac{dC\theta}{k} - \frac{\sqrt{3}dS\theta}{k}\right) \tag{13)–(15}$$

From Eqs. (13) to (15), if the origin point, O, coincides with the mass centre of the body, C, i.e., $d = 0$, then $m_1 = m_2 = m_3 = m/3$, which means that the point masses of the body is distributed equally, and located on the circumference of a circle having radius k.

In mechanism analysis, the links are often considered one-dimensional, e.g., a straight rod, in which its diameter or width and thickness are very small in comparison to length. Considering that the mass lying along the x-axis of local frame, the dynamical equivalence conditions, Eqs. (1)–(4), reduce to

$$\sum_{i=1}^{n} m_i = m; \quad \sum_{i=1}^{n} m_i x_i = m\bar{x}; \quad \sum_{i=1}^{n} m_i x_i^2 = I_c + m\bar{x}^2 \tag{16)–(18}$$

Here also minimum two point-masses are required to represent the one-dimensional link, introducing a total of four variables, i.e., m_1, m_2, x_1, x_2. Specifying any one of the variables, the other three variables can be determined uniquely.

3. Formulation of the balancing problem

The problem of mechanism balancing is formulated as an optimization problem in this section. In order to identify the design variables and constraints a set of equimomental point-masses is defined for each link of mechanism at hand. To calculate the shaking force and shaking moment dynamical equations of motion in minimal set are derived in the parameters of point-masses. These parameters are now treated as design parameters to redistribute the link masses to optimize the shaking force and moment.

3.1. Unconstrained equations of motion

Referring to the ith rigid link, Fig. 2a, of the mechanism, a set of three equimomental point-masses is defined as shown in Fig. 2b. The location of the mass centre, C_i, is defined by vector, $\mathbf{d}_i$ at angle, θ_i, from the axis O_iX_i of the local frame $O_iX_iY_i$ fixed to the link. Link's mass and the mass moment of inertia about O_i are m_i and I_i, respectively. The point-masses, m_{i1}, m_{i2}, m_{i3}, are fixed in local frame, $O_iX_iY_i$, and their distances, l_{i1}, l_{i2}, l_{i3}, and angles, $\theta_{i1}, \theta_{i2}, \theta_{i3}$, are defined from the origin O_i of the link and axis O_iX_i, respectively. Axis O_iX_i is set along the line between O_i and O_{i+1}, that is at angle α_i from the axis OX of the fixed inertial

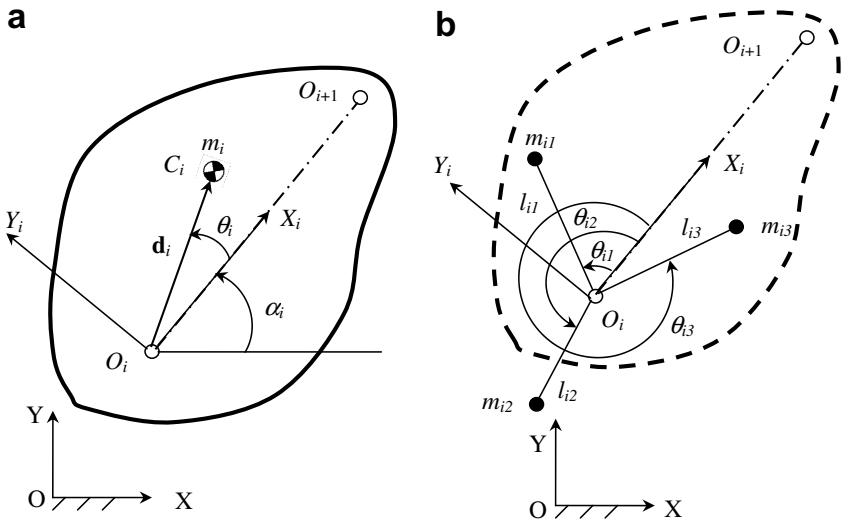

Fig. 2. The ith link: (a) the original link, (b) its equimomental three point-masses system.

frame OXY. Points O_i and O_{i+1} in the link are chosen as the point where the ith link is joined to its surrounding links. All the vectors are represented in the fixed frame, OXY, unless stated otherwise.

If the system of three point-masses is equimomental to the ith link, then it must satisfy the conditions given by Eqs. (5)–(8), i.e.,

$$\sum_j m_{ij} = m_i \tag{19}$$

$$\sum_j m_{ij} l_{ij} C(\theta_{ij} + \alpha_i) = m_i d_i C(\theta_i + \alpha_i) \tag{20}$$

$$\sum_j m_{ij} l_{ij} S(\theta_{ij} + \alpha_i) = m_i d_i S(\theta_i + \alpha_i) \tag{21}$$

$$\sum_j m_{ij} l_{ij}^2 = I_i \tag{22}$$

Note that the first subscript i denotes the link number, and the second subscript $j = 1, 2, 3$, represents point-mass corresponding to the ith link.

Equations of motion, now, are derived using two approaches. One way is to derive equations of motion from rigid body motion. Then the dynamic equivalent conditions are applied to get inertial properties of the links in the parameters of the point masses. An alternate approach is to write the equations motion of point masses. The constrained equations of motion of the system of the point masses are then derived by imposing constraints, i.e., the lengths between the point masses are constants. This approach is given in Appendix A. Here, the first method is adopted. The Newton–Euler (NE) equations [28] of motion for the ith rigid link moving in a plane can be written as

$$\mathbf{M}_i \dot{\mathbf{t}}_i + \mathbf{C}_i \mathbf{t}_i = \mathbf{w}_i \tag{23}$$

where the three-dimensional vectors, $\mathbf{t}_i, \dot{\mathbf{t}}_i$ and $\mathbf{w}_i$, are defined as the twist, twist-rate and wrench of the ith link with respect to the origin, O_i, i.e.,

$$\mathbf{t}_i \equiv \begin{bmatrix} \omega_i \\ \mathbf{v}_i \end{bmatrix}; \quad \dot{\mathbf{t}}_i \equiv \begin{bmatrix} \dot{\omega}_i \\ \dot{\mathbf{v}}_i \end{bmatrix} \quad \text{and} \quad w_i \equiv \begin{bmatrix} n_i \\ \mathbf{f}_i \end{bmatrix} \tag{24}$$

in which ω_i and $\mathbf{v}_i$ are the scalar angular velocity about the axis perpendicular to the plane of motion, and the 2-vector of linear velocity of the origin of the ith link, O_i, respectively. Accordingly, $\dot{\omega}_i$ and $\dot{\mathbf{v}}_i$ are the time

derivatives of the ω_i and $\mathbf{v}_i$, respectively. Also, the scalar, n_i, and the 2-vector, $\mathbf{f}_i$, are the resultant moment about O_i and the resultant force at O_i, respectively. Moreover, the 3×3 matrices, $\mathbf{M}_i$ and $\mathbf{C}_i$ are defined as

$$\mathbf{M}_i \equiv \begin{bmatrix} I_i & -m_i\mathbf{d}_i^{\mathrm{T}}\mathbf{E} \\ m_i\mathbf{E}\mathbf{d}_i & m_i\mathbf{1} \end{bmatrix} \quad \text{and} \quad \mathbf{C}_i \equiv \begin{bmatrix} 0 & \mathbf{0}^{\mathrm{T}} \\ -m_i\omega_i\mathbf{d}_i & \mathbf{O} \end{bmatrix} \tag{25}$$

where $\mathbf{1}$ and $\mathbf{O}$ are the 2×2 identity and zero matrices, respectively, and $\mathbf{0}$ is the 2-vector of zeros, and the 2×2 matrix $\mathbf{E}$ is defined as

$$E \equiv \begin{bmatrix} 0 & -1 \\ 1 & 0 \end{bmatrix}$$

On substitution of the expressions for scalar, I_i, and the 2-vector, $m_i\mathbf{d}_i$, from Eqs. (19)–(22), the 3×3 matrices, $\mathbf{M}_i$ and $\mathbf{C}_i$ are obtained as

$$\mathbf{M}_i \equiv \begin{bmatrix} \sum_j m_{ij}l_{ij}^2 & -\sum_j m_{ij}l_{ij}S(\theta_{ij}+\alpha_i) & \sum_j m_{ij}l_{ij}C(\theta_{ij}+\alpha_i) \\ -\sum_j m_{ij}l_{ij}C(\theta_{ij}+\alpha_i) & \sum_j m_{ij} & 0 \\ \sum_j m_{ij}l_{ij}S(\theta_{ij}+\alpha_i) & 0 & \sum_j m_{ij} \end{bmatrix}; \quad \text{and}$$

$$\mathbf{C}_i \equiv \begin{bmatrix} 0 & 0 & 0 \\ -\omega_i\sum_j m_{ij}l_{ij}C(\theta_{ij}+\alpha_i) & 0 & 0 \\ -\omega_i\sum_j m_{ij}l_{ij}S(\theta_{ij}+\alpha_i) & 0 & 0 \end{bmatrix} \tag{26}$$

Note that the matrices, $\mathbf{M}_i$ and $\mathbf{C}_i$, are applicable for a system n point-masses if $j=1,\ldots,n$. Eq. (26) can be shown to be correct as derived in Appendix A from the Newton's equations of motion valid for the point masses. Note in Eq. (26), that out of nine parameters, m_{ij}, θ_{ij}, l_{ij}, for $j=1,2,3$, for the ith link, five parameters are assigned arbitrarily using the strategy laid down in Section 2, i.e.,

$$\theta_{i1}=0; \quad \theta_{i2}=2\pi/3; \quad \theta_{i3}=4\pi/3; \quad \text{and} \quad l_{i2}=l_{i3}=l_{i1} \tag{27}$$

The other four parameters, namely, m_{i1}, m_{i2}, m_{i3}, and l_{i1}, are then treated as design variables. Equations of motion, Eq. (23), for a mechanism with n moving links are then written as

$$\mathbf{M}\dot{\mathbf{t}} + \mathbf{C}\mathbf{t} = \mathbf{w} \tag{28}$$

where the $3n\times 3n$ matrices, $\mathbf{M}$, and $\mathbf{C}$, are defined as, $\mathbf{M}\equiv \mathrm{diag}[\,\mathbf{M}_1\cdots\mathbf{M}_n\,]$; $\mathbf{C}\equiv \mathrm{diag}[\,\mathbf{C}_1\cdots\mathbf{C}_n\,]$. Also, the $3n$-dimensional generalized twist, twist-rate and wrench vectors, $\mathbf{t}$, $\dot{\mathbf{t}}$ and $\mathbf{w}$, respectively, are

$$\mathbf{t} \equiv \begin{bmatrix} \mathbf{t}_1^{\mathrm{T}} & \cdots & \mathbf{t}_n^{\mathrm{T}} \end{bmatrix}^{\mathrm{T}}; \quad \dot{\mathbf{t}} \equiv \begin{bmatrix} \dot{\mathbf{t}}_1^{\mathrm{T}} & \cdots & \dot{\mathbf{t}}_n^{\mathrm{T}} \end{bmatrix}^{\mathrm{T}}; \quad \text{and} \quad \mathbf{w} \equiv \begin{bmatrix} \mathbf{w}_1^{\mathrm{T}} & \cdots & \mathbf{w}_n^{\mathrm{T}} \end{bmatrix}^{\mathrm{T}}$$

The expressions in the left-hand side of Eq. (28) denote the effective inertial forces and moments, and those on the right-hand side represent the external forces and moments, and those due to the constraints at joints. The $3n$ scalar equations of motion, Eq. (28), for a mechanism having n moving links are referred as unconstrained equations of motion for the mechanism. For example, one has to solve nine equations for a four-bar linkage to find all unknown reactions and driving force. Therefore, determination of the reactions involves lengthy calculations, such as matrix inversion or the solution of simultaneous equations. These calculations are repeated hundreds of time in an optimization code. Hence, it is required to reduce the dimension of the unconstrained equations systematically to a minimal set where one has to solve a less number of equations at a time.

3.2. Constrained equations of motion

Assume that there is one or more closed kinematic loops in a multiloop mechanism. Each closed-loop, Fig. 3, of the mechanism is cut at one of the kinematic joints in order to obtain open-loop system [29]. To

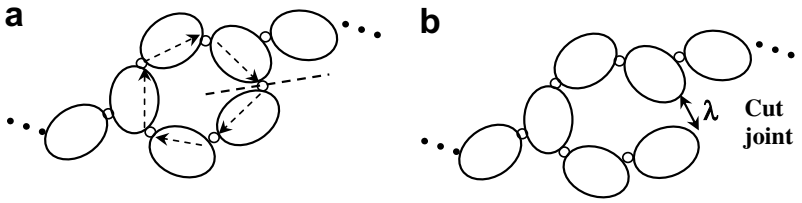

Fig. 3. A closed-loop in multiloop mechanism: (a) the closed loop, (b) its open-loop.

maintain the equilibrium of the mechanism, reaction forces at the cut-joints, referred here as the Lagrange multipliers, are taken as external forces acting on the mechanism.

Decomposing the wrench, $\mathbf{w}_i$, of the ith link into a wrench, $\mathbf{w}_i^{\mathrm{E}}$, of externally applied forces and moments on the ith body by the environment external to the system, and a constraint wrench, $\mathbf{w}_i^{\mathrm{C}}$, of the non-working forces and moments of uncut joints, and $\mathbf{w}_i^{\lambda}$ due to the Lagrange multipliers, i.e., $\mathbf{w}_i \equiv \mathbf{w}_i^{\mathrm{E}} + \mathbf{w}_i^{\mathrm{C}} + \mathbf{w}_i^{\lambda}$, Eq. (28) is rewritten as

$$\mathbf{M}\dot{\mathbf{t}} + \mathbf{C}\mathbf{t} = \mathbf{w}^{\mathrm{E}} + \mathbf{w}^{\mathrm{C}} + \mathbf{w}^{\lambda} \tag{29}$$

Introducing a vector of independent generalized joint coordinates, $\mathbf{q}$, for the open-loop system the generalized twist can be represented as the following linear transformation [30]:

$$\mathbf{t} = \mathbf{N}\dot{\mathbf{q}} \tag{30}$$

where the $3n \times q$ matrix, $\mathbf{N}$ is natural orthogonal complement (NOC) of constraint Jacobian. The matrix $\mathbf{N}$ can be determined using the decoupled orthogonal complement matrices [31]. Pre-multiplication of the transpose of the NOC with the unconstrained NE equations of motion, Eq. (29), leads to a set of constrained equations of motion free from constraint wrenches at the joints other than the cut joints, i.e.,

$$\mathbf{N}^{\mathrm{T}}(\mathbf{M}\dot{\mathbf{t}} + \mathbf{C}\mathbf{t}) = \mathbf{N}^{\mathbf{T}}(w^{\mathrm{E}} + \mathbf{w}^{\lambda}) \tag{31}$$

where $\mathbf{N}^{\mathrm{T}}\mathbf{w}^{C} = \mathbf{0}$ as constraint forces and moment do not perform any work. Eq. (31) can be written as

$$\mathbf{N}^{\mathrm{T}}\mathbf{w}^{*} = \boldsymbol{\tau}^{\mathrm{E}} + \boldsymbol{\tau}^{\lambda} \tag{32}$$

where the $3n$-vector of inertia wrench, $\mathbf{w}^{*} \equiv \begin{bmatrix} \mathbf{w}_1^{*\mathrm{T}} & \cdots & \mathbf{w}_n^{*\mathrm{T}} \end{bmatrix}^{\mathrm{T}}$ is known from input motion, i.e., $\mathbf{w}_i^{*} \equiv \mathbf{M}_i\dot{\mathbf{t}}_i + \mathbf{C}_i\mathbf{t}_i$, $\boldsymbol{\tau}^{\mathrm{E}} \equiv \mathbf{N}^{\mathrm{T}}\mathbf{w}^{\mathrm{E}}$: the q-vector of generalized forces due to external forces and moments; and $\boldsymbol{\tau}^{\lambda} \equiv \mathbf{N}^{\mathrm{T}}\mathbf{w}^{\lambda}$: the q-vector of generalized forces and moments due to the Lagrange multipliers.

Scalar equations of Eq. (32) are linear in a small set of the Lagrange multipliers, and driving forces/torques, which are solvable for given motion. The constraint forces and moments at all the uncut joints then can be determined recursively from the distal links to the first link using the force and moment balance. Unlike conventional approach where the constraint forces and moments, and driving forces and torques are all solved simultaneously, the proposed algorithm solves smaller set of unknowns simultaneously, and rest recursively. The derivation of constrained equations for a multiloop mechanism is illustrated in the next subsection.

3.3. Illustration: the carpet scraping machine mechanism

The carpet scraping machine [32] shown in Fig. 4, is used to clean a carpet after it is woven. It consists of two mechanisms, namely, the Hoeken's four-bar and the Pantograph mechanisms. The Hoeken's mechanism is a crank-rocker mechanism whose coupler generates a partially straight path. The straight line stroke generated by the Hoken's mechanism is magnified by the Pantograph mechanism. The multiloop mechanism has three independent closed loops namely, 1-2-3-8-1, 1-2-5-4-8-1, and 1-2-7-6-4-8-1. Also, note that the links, 1, 3, and 4 are connected to the fixed link, 8. Links, 5 and 7, are not directly connected to each other; they are both joined to 2. In order to open the mechanism, revolute joints between links 3 and 8, 2 and 5, and 2 and 7 of loops 1-2-3-8-1, 1-2-5-4-8-1, and 1-2-7-6-4-8-1, are cut, respectively. Origins of links are defined by O_i, for $i = 1, \ldots, 7$. Because of cutting these joints the Lagrange multipliers, two for each loop, now appear in the open system as indicated in Fig. 5.

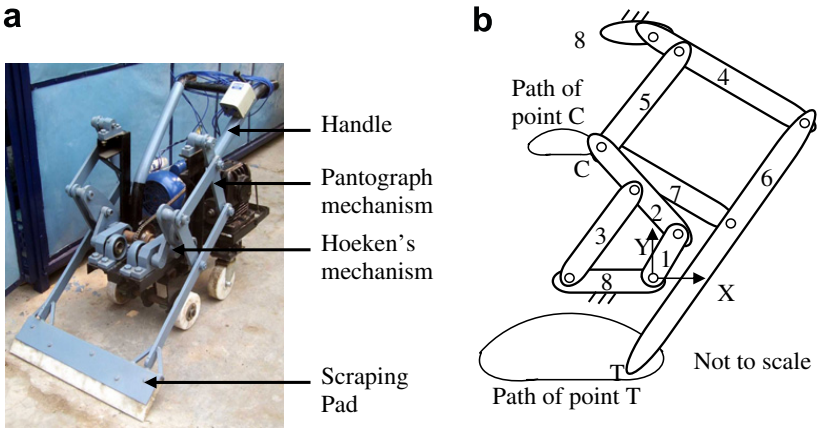

Fig. 4. Carpet scraping machine: (a) photograph [32], (b) multiloop mechanism.

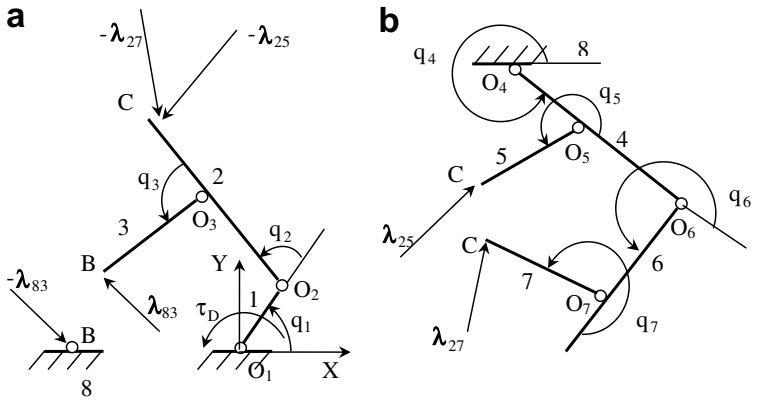

Fig. 5. The open system of the scraping machine mechanism: (a) sub-system I, (b) sub-system II.

Now, these forces are considered as external forces acting on the open system. Because of the open system, the relative joint coordinates, q_i for $i = 1, \ldots, 7$, become independent coordinates. Observing structures of the open system, sub-system I (Fig. 5a) is serial type whereas sub-system II (Fig. 5b) has tree structure. The open system has seven degree-of-freedom. It implies that one can find seven constrained equations of motion in seven unknown, namely, the 2-vectors $\boldsymbol{\lambda}_{83}, \boldsymbol{\lambda}_{25}, \boldsymbol{\lambda}_{27}$ and the scalar τ_D. However, the sub-system II is 4-dof and has four unknowns, namely, the components of 2-vectors $\boldsymbol{\lambda}_{25}, \boldsymbol{\lambda}_{27}$. Hence, its four constrained equations of motions have four unknowns and system of the equation is solvable.

3.3.1. Constrained equations for subsystem II

The four constrained equations of motion, Eq. (32), for subsystem II are now obtained as

$$\mathbf{N}^{\mathrm{T}}\mathbf{w}^{*} = \boldsymbol{\tau}^{\mathrm{E}} + \boldsymbol{\tau}^{\lambda} \tag{33}$$

where the natural orthogonal complement is determined systematically using decoupled natural orthogonal complement (DeNOC) matrices [31]. The 12×4 matrix $\mathbf{N}$ for sub system II is given by

$$\mathbf{N} = \begin{bmatrix} \mathbf{p} & \mathbf{0} & \mathbf{0} & \mathbf{0} \\ \mathbf{A}_{54}\mathbf{p} & \mathbf{p} & \mathbf{0} & \mathbf{0} \\ \mathbf{A}_{64}\mathbf{p} & \mathbf{0} & \mathbf{p} & \mathbf{0} \\ \mathbf{A}_{74}\mathbf{p} & \mathbf{0} & \mathbf{A}_{76}\mathbf{p} & \mathbf{p} \end{bmatrix} \tag{34}$$

where the 3-vector, $\mathbf{p}$, and the 3×3 matrix, $\mathbf{A}_{ij}$, are defined as

$$\mathbf{p} \equiv [\,1 \quad 0 \quad 0\,]^{\mathrm{T}} \quad \text{and} \quad \mathbf{A}_{ij} \equiv \begin{bmatrix} 1 & \mathbf{0}^{\mathrm{T}} \\ -\mathbf{a}_{ij}^{\mathrm{T}}\mathbf{E} & \mathbf{1} \end{bmatrix}$$

respectively, and $\mathbf{0}$ and $\mathbf{1}$ are zero vector and identity matrix of compatible sizes. For the planar motion, $\mathbf{a}_{ij}$ is the 2-vector from the origin of ith link, O_i, to the origin of jth link, O_j.

The vectors of inertia wrench, $\mathbf{w}^* \equiv [(\mathbf{w}_4^*)^{\mathrm{T}}, (\mathbf{w}_5^*)^{\mathrm{T}}, (\mathbf{w}_6^*)^{\mathrm{T}}, (\mathbf{w}_7^*)^{\mathrm{T}}]^{\mathrm{T}}$, and wrench due external forces and moments, $\mathbf{w}^{\mathrm{E}} \equiv [(\mathbf{w}_4^{\mathrm{E}})^{\mathrm{T}}, (\mathbf{w}_5^{\mathrm{E}})^{\mathrm{T}}, (\mathbf{w}_6^{\mathrm{E}})^{\mathrm{T}}, (\mathbf{w}_7^{\mathrm{E}})^{\mathrm{T}}]^{\mathrm{T}}$, are obtained from input motion and external forces acting on the mechanism, respectively. If there are no external forces and moments acting on the mechanism, $\mathbf{w}_4^{\mathrm{E}} = \mathbf{w}_5^{\mathrm{E}} = \mathbf{w}_6^{\mathrm{E}} = \mathbf{w}_7^{\mathrm{E}} = \mathbf{0}$. Similarly, the wrench due to the Lagrange multipliers $\mathbf{w}^{\lambda} \equiv [(\mathbf{w}_4^{\lambda})^{\mathrm{T}}, (\mathbf{w}_5^{\lambda})^{\mathrm{T}}, (\mathbf{w}_6^{\lambda})^{\mathrm{T}}, (\mathbf{w}_7^{\lambda})^{\mathrm{T}}]^{\mathrm{T}}$, where $\mathbf{w}_4^{\lambda}, \mathbf{w}_5^{\lambda}, \mathbf{w}_6^{\lambda}$, and $\mathbf{w}_7^{\lambda}$, are found as

$$\mathbf{w}_4^{\lambda} = \mathbf{0}, \quad \mathbf{w}_5^{\lambda} = \begin{bmatrix} 1 & -\mathbf{a}_{5,C}^{\mathrm{T}}\mathbf{E} \\ \mathbf{0} & \mathbf{1} \end{bmatrix} \begin{bmatrix} 0 \\ \boldsymbol{\lambda}_{25} \end{bmatrix}, \quad \mathbf{w}_6^{\lambda} = \mathbf{0}, \quad \text{and} \quad \mathbf{w}_7^{\lambda} = \begin{bmatrix} 1 & -\mathbf{a}_{7,C}^{\mathrm{T}}\mathbf{E} \\ \mathbf{0} & \mathbf{1} \end{bmatrix} \begin{bmatrix} 0 \\ \boldsymbol{\lambda}_{27} \end{bmatrix} \tag{35}$$

Then the generalized torque, $\boldsymbol{\tau}^{\lambda} = \mathbf{N}^{\mathrm{T}}\mathbf{w}^{\lambda}$, is obtained as

$$\boldsymbol{\tau}^{\lambda} = \begin{bmatrix} -\mathbf{a}_{4,C}^{\mathrm{T}}\mathbf{E}(\boldsymbol{\lambda}_{25} + \boldsymbol{\lambda}_{27}) \\ -\mathbf{a}_{5,C}^{\mathrm{T}}\mathbf{E}\boldsymbol{\lambda}_{25} \\ -\mathbf{a}_{6,C}^{\mathrm{T}}\mathbf{E}\boldsymbol{\lambda}_{27} \\ -\mathbf{a}_{7,C}^{\mathrm{T}}\mathbf{E}\boldsymbol{\lambda}_{27} \end{bmatrix} \tag{36}$$

where the Langrage multipliers have two components, namely, $\boldsymbol{\lambda}_{25} \equiv [\lambda_{25x}, \lambda_{25y}]^{\mathrm{T}}$, and so on. The four constrained equations, Eq. (33), are now solved for four scalar multipliers, namely, λ_{25x}, λ_{25y}, λ_{27x}, and λ_{27y}. These multipliers are then the known external forces in subsystem I.

3.3.2. Constrained equations for subsystem I

In the next step, for sub system I the 9×3 matrix $\mathbf{N}$ is given by

$$N = \begin{bmatrix} \mathbf{p} & \mathbf{0} & \mathbf{0} \\ \mathbf{A}_{21}\mathbf{p} & \mathbf{p} & \mathbf{0} \\ \mathbf{A}_{31}\mathbf{p} & \mathbf{A}_{32}\mathbf{p} & \mathbf{p} \end{bmatrix} \tag{37}$$

$\mathbf{w}^* \equiv [(\mathbf{w}_1^*)^{\mathrm{T}}, (\mathbf{w}_2^*)^{\mathrm{T}}, (\mathbf{w}_3^*)^{\mathrm{T}}]^{\mathrm{T}}$, and $\mathbf{w}^{\mathrm{E}} \equiv [(\mathbf{w}_1^{\mathrm{E}})^{\mathrm{T}}, (\mathbf{w}_2^{\mathrm{E}})^{\mathrm{T}}, (\mathbf{w}_3^{\mathrm{E}})^{\mathrm{T}}]^{\mathrm{T}}$. Hence, the 3-vectors of generalized torques of external forces and Lagrange multipliers, respectively, are obtained as

$$\boldsymbol{\tau}^{\mathrm{E}} = \begin{bmatrix} \tau_D + \mathbf{a}_{1,C}^{\mathrm{T}}\mathbf{E}(\boldsymbol{\lambda}_{25} + \boldsymbol{\lambda}_{27}) \\ +\mathbf{a}_{2,C}^{\mathrm{T}}\mathbf{E}(\boldsymbol{\lambda}_{25} + \mathbf{f}_{27}) \\ 0 \end{bmatrix} \quad \text{and} \quad \boldsymbol{\tau}^{\lambda} = \begin{bmatrix} -\mathbf{a}_{1,B}^{\mathrm{T}}\mathbf{E}\boldsymbol{\lambda}_{83} \\ -\mathbf{a}_{2,B}^{\mathrm{T}}\mathbf{E}\boldsymbol{\lambda}_{83} \\ -\mathbf{a}_{3,B}^{\mathrm{T}}\mathbf{E}\boldsymbol{\lambda}_{83} \end{bmatrix} \tag{38}$$

Thus the constrained equations obtained from Eqs. (37) and (38) can be solved for three unknowns, λ_{83x}, λ_{83y}, and τ_D. Rest of the reactions, i.e., $\mathbf{f}_{67}, \mathbf{f}_{46}, \mathbf{f}_{45}$ and $\mathbf{f}_{84}$ in sub-system II, and $\mathbf{f}_{23}, \mathbf{f}_{12}$ and $\mathbf{f}_{81}$, in sub-system I are finally solved recursively. Thus, dynamic analysis for the constraint forces of the multiloop mechanism is carried out with maximum of four simultaneous equations only, whereas conventional approach [33] would require the solution of twenty one simultaneous equations.

3.4. Shaking force and shaking moment

Fig. 6 shows n moving links of a multiloop linkage in which fixed link, $(n+1)$st, is detached by applying reaction forces and moments of it on moving links. Amongst n moving links, let assume that p links are connected to the fixed link. The shaking force is then defined as the vector sum of the inertia forces associated with the mechanism, and the shaking moment is the sum of the inertia couples and the moment of the inertia forces

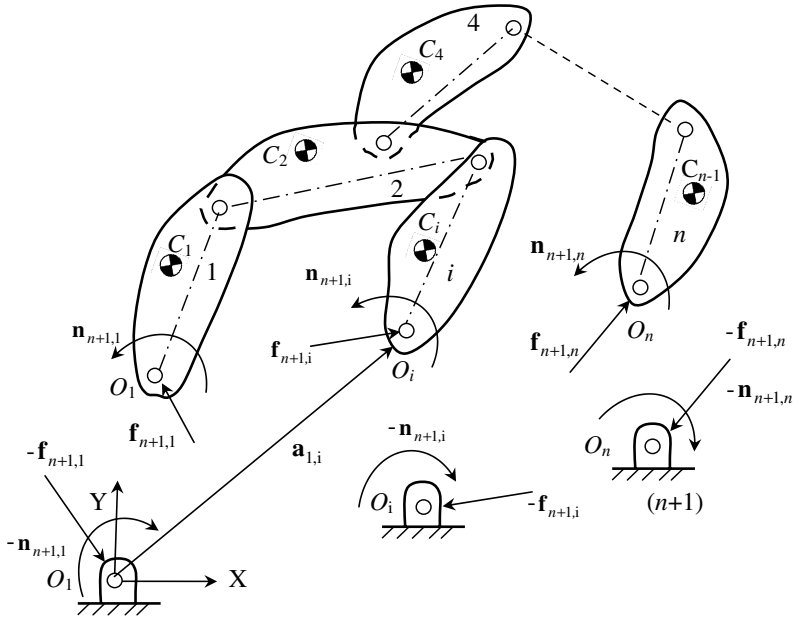

Fig. 6. A multiloop mechanism.

[13,23]. By the definitions, the shaking force, and the shaking moment with respect to O_1, transmitted to the fixed link are the reaction of the resultant inertia forces and moments of the mechanism, respectively, i.e.,

$$\mathbf{f}_{\mathrm{sh}} = -\sum_{i=1}^{n} \mathbf{f}_i^*; \quad \text{and} \quad n_{\mathrm{sh}} = -\sum_{i=1}^{n} (n_i^* - \mathbf{a}_{1,i}^{\mathrm{T}} \mathbf{E} \mathbf{f}_i^*) \tag{39}$$

where n_i^* and $\mathbf{f}_i^*$ are inertia moment and the 2-vector of inertia force, respectively, acting at and about origin O_i of the ith body and they are component of $\mathbf{w}_i^*$. The 2-vector $\mathbf{a}_{1,i}$ is defined from O_1 to origin of the ith link as shown in Fig. 6.

Substituting the resultant force and moment in terms of external force and moment, and reactions due to the adjoining joints, the NE equations of motion, Eq. (23), for the ith link are rewritten as

$$\mathbf{f}_i^* = \mathbf{f}_i^{\mathrm{e}} + \sum_{k} \mathbf{f}_{ki}; \quad \text{and} \quad n_i^* = n_i^{\mathrm{e}} + \sum_{k} (n_{ki} - \mathbf{a}_{ik}^{\mathrm{T}} \mathbf{E} \mathbf{f}_{ki}) \tag{40}$$

where $\mathbf{f}_{ki}$ and n_{ki} are the bearing reaction force and moment on the ith link by the kth link, respectively. Furthermore, $\mathbf{f}_i^{\mathrm{e}}$ and n_i^{e} are the external force and moment acting at and about origin, O_i, respectively. Note that origin for the ith link is defined at the joint where it is coupled the ith link with its previous link. Also, twist, twist-rate, and inertia force and torque are also defined at this point. Vector $\mathbf{a}_{ik}$ is defined from the origin of the ith link to the joint where the kth link is connected. Note that the driving torques and/or forces are taken as external torques and/or forces. Now, using, Eqs. (40), the shaking force, and the shaking moment w.r.t. to O_1 transmitted to the fixed link are obtained as

$$\mathbf{f}_{\mathrm{sh}} = -\sum_{j=1}^{p} \mathbf{f}_{n+1,j} - \sum_{i=1}^{n} \mathbf{f}_i^{\mathrm{e}}; \quad \text{and} \quad n_{\mathrm{sh}} = -\sum_{j=1}^{p} (n_{n+1,j} - \mathbf{a}_{1,j}^{\mathrm{T}} \mathbf{E} \mathbf{f}_{n+1,j}) - \sum_{i=1}^{n} (n_i^{\mathrm{e}} - \mathbf{a}_{1,i}^{\mathrm{T}} \mathbf{E} \mathbf{f}_i^{\mathrm{e}}) \tag{41}$$

where $\mathbf{f}_{n+1,j}$ represents the reaction force on the jth link by the fixed link, where $j = 1,\ldots,p$. For all links not connected with the fixed link, i.e., $p < i \leqslant n$, the term $\mathbf{f}_{n+1,j}$ is zero. The dynamic quantities, e.g., shaking force, shaking moment, bearing reactions, and design variables are of different units and magnitudes. In order to harmonize them, the original mechanism is made dimensionless by normalizing the parameters as follows:

$a_{ij} := a_{ij}/a_1$ Normalized distance between joints i and j; where $a_1 \equiv a_{12}$
$d_i := d_i/a_1$ Normalized distance of the mass centre from the ith link origin
$m_i := m_i/m_1^{\mathrm{o}}$ Normalized mass of the ith link
$I_i := I_i/(m_1^{\mathrm{o}} a_1^2)$ Normalized moment of inertia of the ith link w.r.t. its origin, O_i

The dynamic quantities are based on forces and moments non-dimensionalized with respect to the original mechanism parameters and input speed as typically suggested in the literature [35]. They are defined as

$f := f/(m_1^{\mathrm{o}} a_1 \omega_1^2)$ Definition of normalized force to any force, f

$n := n/(m_1^{\mathrm{o}} a_1^2 \omega_1^2)$ Definition of normalized moment to any moment, n

where f is the magnitude of vector $\mathbf{f}$. Superscript 'o' is used for those parameters of the original mechanism whose values are varying in the optimization.

3.5. Optimality criterion

There are many possible criteria by which the shaking force and shaking moment transmitted to the fixed link of the mechanism can be minimized. For example, one criterion could be the root-mean-square (RMS) of shaking force, shaking moment, and required input-torque for given motion, and/or combination of these. Besides RMS values there are other ways to specify the dynamic quantities, namely, by maximum values, or by the amplitude of the specified harmonics, or by the amplitudes at certain point in the cycle. The choice of course depends on the requirements. Here, the RMS value is preferred over others as it gives equal emphasis on the results of every time instances of the cycle, and every harmonic component. The root mean square (RMS) values of the normalized shaking force, f_{sh}, and the normalized shaking moment, n_{sh}, at p discrete positions of the mechanism are defined as

$$\tilde{f}_{\mathrm{sh}} \equiv \frac{1}{p}\sqrt{\sum f_{\mathrm{sh}}^2}; \quad \text{and} \quad \tilde{n}_{\mathrm{sh}} \equiv \frac{1}{p}\sqrt{\sum n_{\mathrm{sh}}^2} \tag{42}$$

where $\tilde{f}_{\mathrm{sh}}$ and $\tilde{n}_{\mathrm{sh}}$ are the RMS values of the normalized shaking force and the normalized shaking moment, respectively. Now, optimality criteria can be weighted sum of competing dynamic quantities, namely, shaking force, shaking moment, input-torque and the reactions due to the frame of mechanism. However, it obvious from Eq. (41) that the shaking force and shaking moment include the frame reactions and the input-torque, respectively. Hence, it is sufficient to form optimality criteria as weighted sum the shaking force and shaking moment. Considering the RMS values of the normalized shaking force and shaking moment, an optimality criterion is proposed as

$$z = w_1 \tilde{f}_{\mathrm{sh}} + w_2 \tilde{n}_{\mathrm{sh}} \tag{43}$$

Moreover, w_1 and w_2 are weighting factors whose values may vary depending on application. For example, $w_1 = 1.0$ and $w_2 = 0$ if the objective is to minimize the shaking force only.

3.6. Design variables and constraints

Based on the dynamic analysis presented in Sections 3.1 and 3.2, shaking force and shaking moment are formulated in link parameters, $m_{ij}, \theta_{ij}, l_{ij}$ for $j = 1, 2, 3$. Amongst them, five parameters are assigned arbitrarily according to Eq. (27). The remaining four parameters, namely, m_{i1}, m_{i2}, m_{i3}, and l_{i1}, for each link are considered as the design variables (DV). Finally, for a mechanism having n moving links, the shaking force and shaking moment are obtained as function of design variables, i.e.,

$$\tilde{f}_{\mathrm{sh}} = f_1(\mathbf{x}); \quad \text{and} \quad \tilde{n}_{\mathrm{sh}} = f_2(\mathbf{x}) \tag{44}$$

where the $4n$-dimensional vector, $\mathbf{x}$, of the design variables for the normalized mechanism is defined as follows:

$$\mathbf{x} \equiv [m_{11}, m_{12}, m_{13}, l_{11}, \cdots, m_{n1}, m_{n2}, m_{n3}, l_{n1}]^{\mathrm{T}} \tag{45}$$

The minimum mass, $m_{i,\min}$, and its distribution of the ith link can be decided by the strength of material. Furthermore, Maximum mass, $m_{i,\max}$, can be taken according to what extent the shaking force and shaking moment eliminated. Now, the optimization problem is posed as

$$\underset{\text{w.r.t. } \mathbf{x}}{\text{Minimize}}\, z(\mathbf{x}) = w_1 \tilde{f}_{\text{sh}} + w_2 \tilde{n}_{\text{sh}} \tag{46a}$$

$$\text{Subject to } m_{i,\min} \leqslant (m_{i1} + m_{i2} + m_{i3}) \leqslant m_{i,\max}; \tag{46b}$$

$$l_{i1,\min} \leqslant l_{i1} \leqslant l_{i1,\max} \quad \text{for} \quad i = 1, \ldots, n. \tag{46c}$$

where $l_{i1,\min_1}$ and $l_{i1,\max}$ are bounds on the distances of point-masses. The feasible region of the design space is defined by Eqs. (46b) and (46c).

4. Numerical examples

The flexibility and effectiveness of the proposed optimization problem formulation, as proposed in Section 3, is demonstrated with help of Hoeken's four-bar and the multiloop mechanism used in the carpet scraping machine shown in Fig. 4.

4.1. Example 1: Hoeken's four-bar mechanism

The normalized link parameters of the original Hoeken's four-bar mechanism, Fig. 7, used in the carpet scraping machine are given in Table 1. All the parameters are made dimensionless w.r.t. the parameters of the 1st link. The equimomental point-masses for each link are obtained using Eqs. (19)–(22), which are given in Table 2. To find the effect of inertia-induced forces and moments, it is assumed that no external forces and moments acting other than the driving torque. Then the shaking force and shaking moment are obtained using Eq. (41) for the mechanism as

$$\mathbf{f}_{\text{sh}} = -(\mathbf{f}_{41} + \mathbf{f}_{43}) \quad \text{and} \quad n_{\text{sh}} = -(n_{41} + n_{43} - \mathbf{a}_{13}^{\text{T}} \mathbf{E} \mathbf{f}_{43} + n_1^{\text{e}}) \tag{47}$$

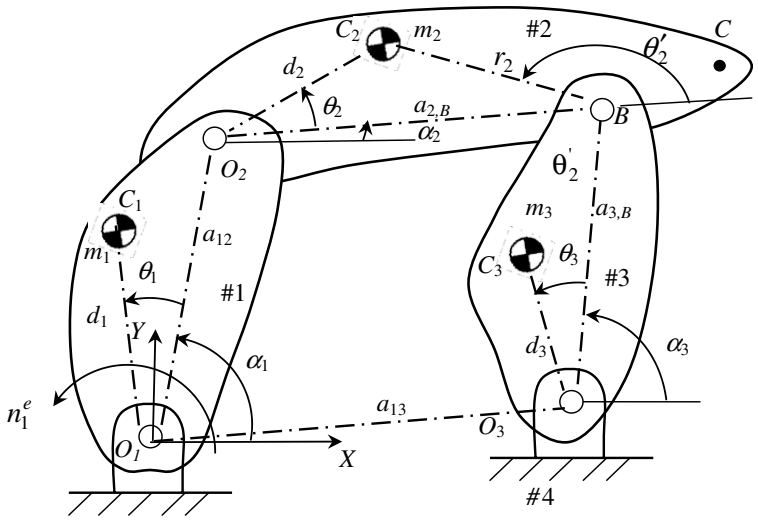

Fig. 7. A Hoeken's four-bar mechanism.

Table 1
Parameters of the normalized original Hoeken's mechanism

Link i	1	2	3
Link length, a_{ik}	1	3.02	3.02
Link mass, m_i^{o}	1	7.100	1.900
Center of mass location, d_i^{o}	0.15	2.86	1.25
Center of mass location, θ_i^{o} (°)	0	0	0
Moment of inertia, I_i^{o}	0.4023	84.4028	5.8299

$O_1O_2 = a_{12} = 0.038$ m; $m_1^{\text{o}} = 0.326$ kg; $O_1O_3 = a_{13} = 2.35$ @ 0°; $\omega_1 = 1$ rad/s.

Table 2
Equivalent point-masses of the normalized Hoeken's mechanism

Link i	1	2	3
Point-mass, m^{o}_{i1}	0.4910	6.2930	1.5372
Point-mass, m^{o}_{i2}	0.2545	0.4035	0.1814
Point-mass, m^{o}_{i3}	0.2545	0.4035	0.1814
Location of point-masses, l^{o}_{i1}	0.6343	3.4479	1.7517

where n^{e}_{1} is the driving torque applied to the link #1. Since all joints in the mechanism are revolute, $n_{41} = n_{12} = n_{23} = n_{43} = 0$. In order to know effect of force balancing, the optimization problem of the mechanism balancing is first formulated as force balancing problem.

4.1.1. Shaking force balancing

The effectiveness of the balancing method proposed in Section 3 is compared with the analytical balancing method proposed by Berkof and Lowen [2]. Berkof and Lowen found balancing conditions for the total force balance of a general four-bar linkage by redistributing its masses. The method is based on making the mass centre of a mechanism stationary called as the method of linearly independent vectors. The conditions for the total force balance for a four bar linkage are as follows:

$$m_1 d_1 = m_2 r_2 \frac{a_{12}}{a_{2,B}}, \quad \text{and} \quad \theta_1 = \theta'_2; \quad m_3 d_3 = m_2 d_2 \frac{a_{3,B}}{a_{2,B}}, \quad \text{and} \quad \theta_3 = \theta_2 + \pi \tag{48}$$

where point B is the location of joint between links, 2 and 3, and all the link parameters are shown in Fig. 7. In Eq. (48), there are nine unknowns, d_i, θ_i, and m_i for $i = 1, 2, 3$, and only four equations. If the parameters of link 2 are prescribed then angles θ_1 and θ_3 can be found. This determines the radial lines on which the centres of mass of links 1 and 3 must be placed. Therefore, only product of mass and distance, $m_1 d_1$ and $m_3 d_3$, may be found.

To compare results obtained from the proposed method in this paper with that of the analytical method, Eq. (48), parameters of link 2 are assumed to be its original. The parameters of the remaining two links, 1 and 3, form an eight-dimensional design vector, $\mathbf{x}$, as $\mathbf{x} \equiv [m_{11}, m_{12}, m_{13}, l_{11}, m_{31}, m_{32}, m_{33}, l_{31}]^{T}$. Considering three cases: (1) $m_i = 1$; (2) $m_i = 2$; and (3) $m_i = 5$ with $l_{i1} = l^{\circ}_{i1}$ for the analysis, the problem of shaking force balancing is formed as follows:

$$\text{Minimize } z = \tilde{f}_{\text{sh}} \tag{49a}$$

$$\text{Subject to } m_{i1} + m_{i2} + m_{i3} = m_i; \quad \text{for } i = 1, 3 \tag{49b}$$

In case (1) the masses of links, 1 and 3, are kept same as those in the original mechanism. Similarly, in cases (2) and (3), link masses are increased to twice and five times, respectively. Optimization tool box of MATLAB [34] is used to solve the problem posed in Eq. (49). The optimized results for the point-masses, and the geometry of links obtained from them are given in Table 3. Angles, θ_i, and mass–distance products, $m_i d_i$, for $i = 1, 3$, are

Table 3
Optimized values for point-masses and links geometries

Cases	Link i	Point-masses			Total mass m_i	Centre mass location		Mass–distance product $m_i d_i$
		m_{i1}	m_{i2}	m_{i3}		d_i	θ_i (°)	
(1)	1	−0.0619	0.5309	0.5309	1.000	0.3761	**180.00**	**0.3760**
	3	−2.3466	1.4929	1.4929	1.900	10.6870	**180.00**	**20.3064**
(2)	1	0.2715	0.8643	0.8643	2.000	0.1880	**180.00**	**0.3760**
	3	−6.4616	5.1308	5.1308	3.800	5.3438	**180.00**	**20.3064**
(3)	1	1.2715	1.8643	1.8643	5.000	0.0752	**180.00**	**0.3760**
	3	−4.5616	7.0308	7.0308	9.500	2.1375	**180.00**	**20.3064**

Values using Berkof and Lowen conditions: $m_1 d_1 = 0.3762$; $m_3 d_3 = 20.3060$ and $\theta_1 = 180°$; $\theta_3 = 180°$.

Table 4
Comparison of the RMS values of dynamic quantities between the original and the force-balanced Hoeken's mechanism

Mechanism	Bearing reaction forces				Input-torque	Shaking force	Shaking moment
	$\tilde{f}_{41}$	$\tilde{f}_{12}$	$\tilde{f}_{23}$	$\tilde{f}_{43}$	$\tilde{\tau}$	$\tilde{f}_{\mathrm{sh}}$	$\tilde{n}_{\mathrm{sh}}$
Original	24.7783	24.6928	22.9319	23.0385	15.3173	**11.5362**	36.7785
Case (1)	24.4813	24.6928	22.9320	24.4812	15.3174 (00)	**1.11E−5(−100)**	40.2375 (09)
Case (2)	26.1312	26.3421	24.3354	26.1312	16.3560 (07)	**1.11E−5(−100)**	42.8985 (17)
Case (3)	31.1002	31.3095	28.7244	31.1002	19.4858 (27)	**1.11E−5(−100)**	50.8993 (38)

The value in parenthesis denotes percent increment over the corresponding values of the original mechanism in the columns.

shown in the last two columns. The results obtained by the proposed formulation are in good agreement with the analytical results which are shown in Table 3.

The normalized shaking forces in all cases are reduced to negligible in comparison to that in the original mechanism, as shown in Table 4. As expected, the RMS values of the normalized shaking moment, the input-torque, and bearing reactions in the joints increase with the link masses. For example, the shaking moment increases by 38% over the corresponding values of the original mechanism in case (3). Similarly, Table 4 shows increment in the bearing reactions also.

4.1.2. Optimization of shaking force and moment

The effect of force balancing on bearing reactions, input-torque, and the shaking moment in a family of four-bar linkages is investigated by Lowen et al. [4]. They had shown that the bearing reactions, input-torque as well as the shaking moment increase up to 50 percent in most of the case. This fact is also clear from the results of the previous section. The conclusions of Lowen et al. [4] and other researchers suggest that only force balancing is not effective, and the balancing of mechanism requires trade-off among various dynamic quantities. In this paper, the optimality criteria proposed in Eq. (43) is used which combine both the shaking force and shaking moment. The constraints on the design variables, namely, m_{i1}, m_{i2}, m_{i3}, and l_{i1}, for $i = 1, 2, 3$, are depend on application.

In this study, two sets of constraints on the design variables are considered, namely, (a) total mass of each link and the distances of point-masses from the link's origin are constrained. Here negative values of the point-masses are allowed; and (b) in addition to the constraints in (a), negative values of the point-masses are not allowed. For the both problems, θ_{i1}, θ_{i2}, and θ_{i3} are 0, $2\pi/3, 4\pi/3$ and $l_{i2} = l_{i3} = l_{i1}$ are assigned as an equimomental conditions. Then design vector, $\mathbf{x}$, consists of a total of 12 design variables, m_{ij} and l_{i1} for $i = 1, 2, 3$, is defined as

$$\mathbf{x} \equiv [m_{11}, m_{12}, m_{13}, l_{11}, m_{21}, m_{22}, m_{23}, l_{21}, m_{31}, m_{32}, m_{33}, l_{31}]^{\mathrm{T}}.$$

The optimization problem is then posed as

$$\text{Minimize } z = w_1 \tilde{f}_{\mathrm{sh}} + w_2 \tilde{n}_{\mathrm{sh}} \tag{50a}$$

$$\text{(a) Subject to } m_i^{\mathrm{o}} \leqslant (m_{i1} + m_{i2} + m_{i3}) \leqslant 5m_i^{\mathrm{o}} \tag{50b}$$

$$0.5l_i^{\mathrm{o}} \leqslant l_{i1} \leqslant 1.5l_i^{\mathrm{o}}; \quad \text{for } i = 1, 2, 3 \tag{50c}$$

$$\text{(b) Subject to } m_i^{\mathrm{o}} \leqslant (m_{i1} + m_{i2} + m_{i3}) \leqslant 5m_i^{\mathrm{o}} \tag{50d}$$

$$0.5l_i^{\mathrm{o}} \leqslant l_{i1} \leqslant 1.5l_i^{\mathrm{o}} \tag{50e}$$

$$m_{i1}, m_{i2}, m_{i3} \geqslant 0; \quad \text{for } i = 1, 2, 3 \tag{50f}$$

Choosing three set of weighting factors (w_1, w_2): $(1, 0)$, $(0.5, 0.5)$, and $(0, 1)$, total six cases are investigated. Table 5 shows the design vector obtained for each case. The geometry and inertial properties of the mechanism for each case are obtained back from the design vector using Eqs. (19)–(22), and given in Table 6. Figs. 8 and 9 show a comparison to the dynamic quantities with those of the original mechanism. The figures clearly demonstrates that cases, a(2) and b(2), are effective for the first and second sets of constraints, respectively. Table 7

Table 5
Design vector for the balanced Hoken's mechanism

Case: (w_1, w_2)	Design vector, **x**
Case a(1): (1.0, 0.0)	$[-3.5246\ \ 2.3285\ \ 2.3718\ \ 0.9134\ \ 4.3784\ \ 1.3282\ \ 1.3968\ \ 1.7398\ \ -2.9843\ \ 2.5052\ \ 2.3818\ \ 0.9667]^T$
Case a(2): (0.5, 0.5)	$[-4.8784\ \ 0.7227\ \ 5.1566\ \ 0.5886\ \ 5.2843\ \ -1.3781\ \ 3.1938\ \ 1.7240\ \ -5.1095\ \ 8.0046\ \ -0.9951\ \ 0.8759]^T$
Case a(3): (0.0, 1.0)	$[0.4910\ \ 0.2545\ \ 0.2545\ \ 0.6343\ \ 5.0594\ \ 0.7484\ \ 1.2922\ \ 1.7240\ \ -2.9119\ \ 8.3848\ \ -3.5729\ \ 0.8759]^T$
Case b(1): (1.0, 0.0)	$[0\ \ 2.3350\ \ 2.6650\ \ 0.9514\ \ 5.9063\ \ 0.3106\ \ 0.8831\ \ 2.4240\ \ 0\ \ 4.9305\ \ 4.5695\ \ 2.6276]^T$
Case b(2): (0.5, 0.5)	$[01.5990\ \ 3.4010\ \ 0.9514\ \ 4.6933\ \ 0\ \ 2.4067\ \ 1.7240\ \ 09.5000\ \ 0\ \ 0.8759]^T$
Case b(3): (0.0, 1.0)	$[0.4910\ \ 0.2545\ \ 0.2545\ \ 0.6343\ \ 4.9665\ \ 0\ \ 2.1335\ \ 1.7240\ \ 0\ \ 9.5000\ \ 0\ \ 0.9368]^T$

Table 6
Geometry and moment of inertia of the balanced Hoken's mechanism

Case	Link, i	Total link mass m_i	Centre mass location		Moment of inertia I_i
			d_i	θ_i (°)	
Case: a(1)	1	1.176	4.5642	180.36	0.9809
	2	7.103	0.7388	358.87	21.5013
	3	1.903	2.7582	178.87	1.7781
		10.182			
Case: a(2)	1	1.000	5.1222	206.16	0.3468
	2	7.100	1.4330	317.86	21.1024
	3	1.900	5.3554	137.86	1.4577
		10.000			
Case: a(3)	1	1.000	0.1500	0.00	0.4023
	2	7.100	0.9874	353.35	21.1024
	3	1.900	5.3666	117.18	1.4577
		10.000			
Case: b(1)	1	5.000	0.4788	186.52	4.5258
	2	7.100	1.8206	354.66	41.7180
	3	9.500	1.3166	176.23	65.5907
		21.600			
Case: b(2)	1	5.000	0.5608	211.97	4.5258
	2	7.100	0.9870	329.15	21.1024
	3	9.500	0.8759	120.00	7.2884
		21.600			
Case: b(3)	1	1.000	0.1500	0.00	0.4023
	2	7.100	1.0478	334.65	21.1024
	3	9.500	0.9368	120.00	8.3371
		17.600			

shows comparison to the RMS values of the normalized dynamic quantities occurring motion cycle with those of the original mechanism. The following conclusions are accrued by comparison of the results given in Tables 5–7.

Magnitudes of the shaking force and shaking moment occurred during motion cycle are minimum when equal weight is given to both the quantities as shown by bold numbers in Table 7.

Total mass of the mechanism is minimum or increase very little in cases a(1)–a(3), whereas it increases two-fold or more in cases b(1)–b(3). This is because point-masses may take negative value in problem (a). This is obtained at a cost of displacing the centres of masses of links far away from the designed link origins. For example, in cases a(2) and b(2), the location of the mass centre of link 3, i.e., d_3, is 5.3554 and 0.8759, respectively, which are about 4.2 and 0.7 times higher than that of its original value 1.25.

It is not necessary that the point-masses are positives. The conditions, that a set of positive and negative point-masses represent a realizable link, are the total mass and moment of inertia about axes through the

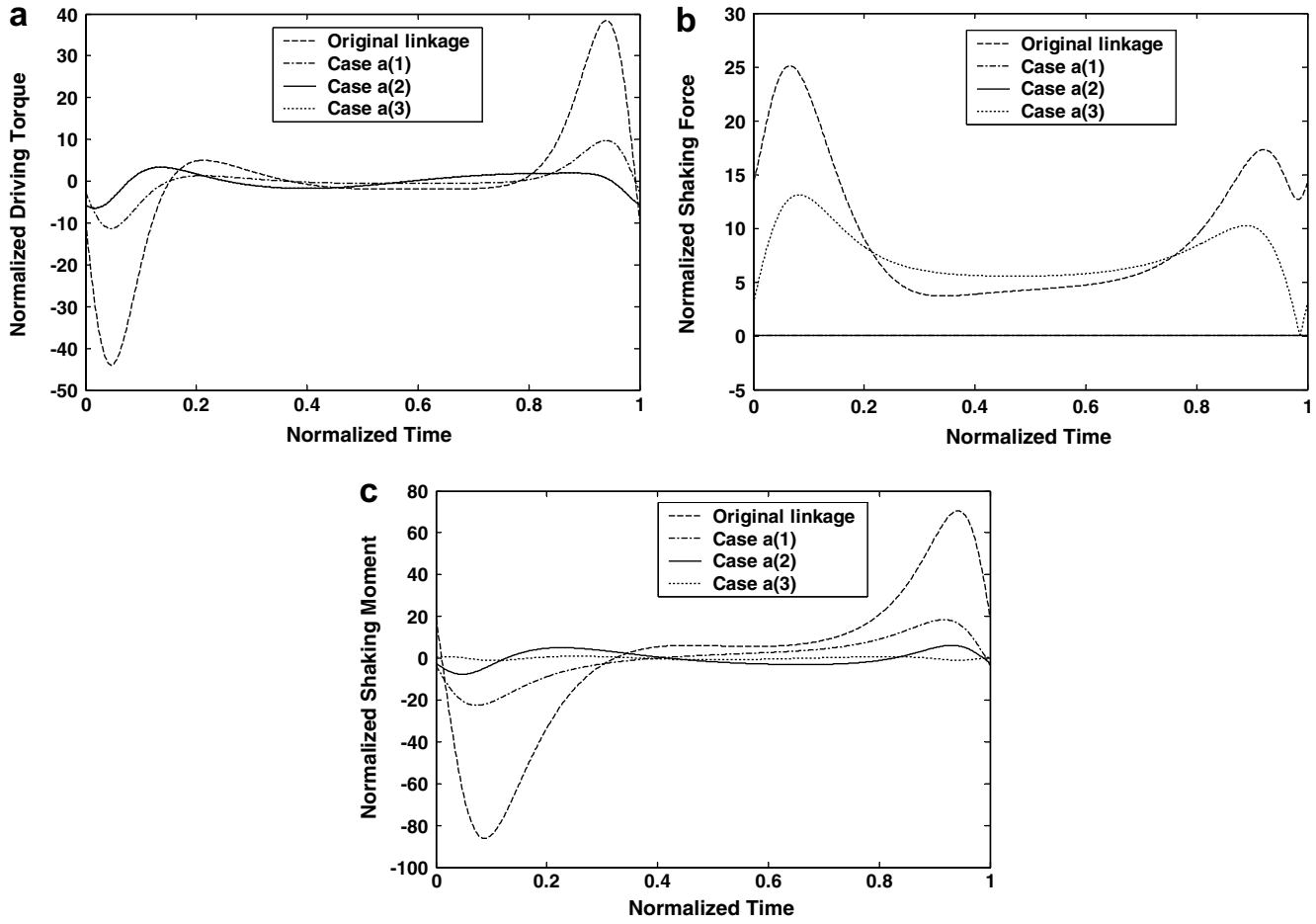

Fig. 8. Dynamic performance of the Hoeken's mechanism, case (a) normalized driving torque, (b) normalized shaking force, (c) normalized shaking moment to fixed point O_1.

centre of mass must be positive. Non-negativity of the total mass of each link is achieved by constraining it as $m_i^o \leqslant (m_{i1} + m_{i2} + m_{i3}) \leqslant 5m_i^o$. Non-zero moment of inertia are achieved by assuming, $l_{i2} = l_{i3} = l_{i1}$ and restricting l_{i1} as $0.5l_i^o \leqslant l_{i1} \leqslant 1.5l_i^o$.

The balanced geometry obtained in case a(1), which is only shaking force balancing as discussed in Section 4.1.1, satisfy the analytical conditions, Eq. (48). With the optimization method proposed, it is not necessary to assume some parameters and calculate others. It optimizes distribution of masses of all the links.

4.2. Example 2: the carpet scraping machine mechanism

Dynamic analysis of the carpet scraping machine mechanism is shown in Section 3.2. Here the proposed method is used to optimize its shaking force and shaking moment. Table 8 defines its geometry, masses, and inertia of the normalized original mechanism. The shaking force and shaking moment of the mechanism are obtained, using Eq. (41), as

$$\mathbf{f}_{\text{sh}} = -(\mathbf{f}_{81} + \mathbf{f}_{83} + \mathbf{f}_{84}) \tag{51}$$

$$n_{\text{sh}} = -(n_{81} + n_{83} + n_{84} - \mathbf{a}_{1B}^{\text{T}}\mathbf{E}\mathbf{f}_{83} - \mathbf{a}_{14}^{\text{T}}\mathbf{E}\mathbf{f}_{84} + n_1^{\text{e}}) \tag{52}$$

where n_1^{e} is driving torque applied to the link #1. Since all the joints in the mechanism are revolute, $n_{81} = n_{82} = n_{84} = 0$. Based on the discussion in Section 3, m_{i1}, m_{i2}, m_{i3}, and l_{i1}, for $i = 1, \ldots, 7$, are chosen as the design variables for the problem. The parameters, θ_{i1}, θ_{i2}, and θ_{i3} are 0, $2\pi/3$, $4\pi/3$ and $l_{i2} = l_{i3} = l_{i1}$

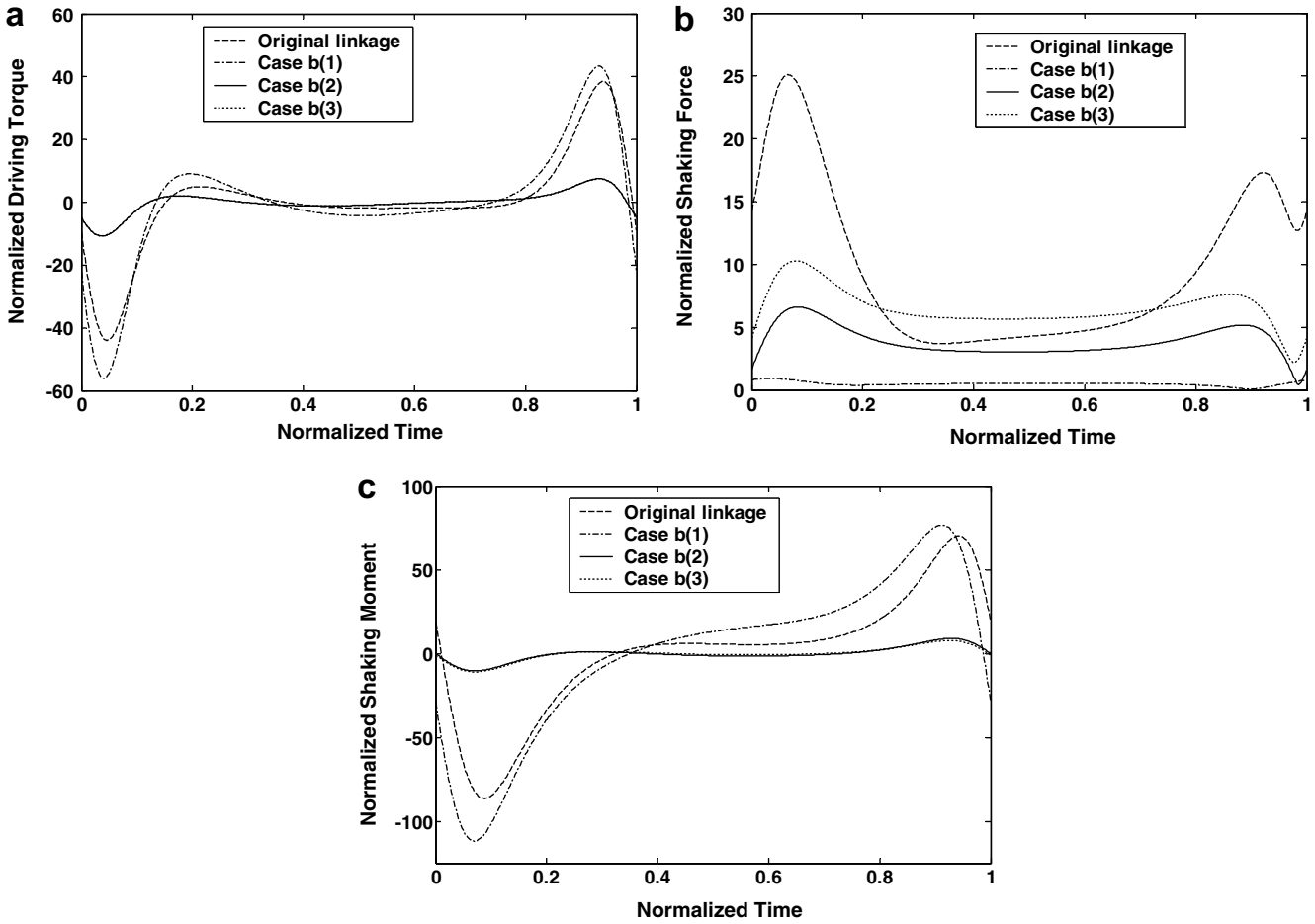

Fig. 9. Dynamic performance of the Hoeken's mechanism, case (b), (a) normalized driving torque, (b) normalized shaking force, (c) normalized shaking moment to fixed point O_1.

Table 7
Comparison of the RMS values of dynamic quantities between the original and the balanced Hoken's mechanism

Case	Bearing reactions				Input-torque $\tilde{\tau}$	Shaking force $\tilde{f}_{sh}$	Shaking moment $\tilde{n}_{sh}$
	$\tilde{f}_{41}$	$\tilde{f}_{12}$	$\tilde{f}_{23}$	$\tilde{f}_{43}$			
Original mechanism	24.7783	24.6928	22.9319	23.0385	15.3173	**11.5362**	36.7785
Optimization problem (a)							
Case: a(1)	6.2614	10.2671	5.8774	6.2615	3.9129	5.98E−5	10.2544
					(−75)	(−100)	(−72)
Case: a(2)	**4.5516**	**6.8703**	**3.9930**	**4.5518**	**2.1480**	**4.46E−4**	**3.4903**
					(−86)	**(−100)**	**(−91)**
Case: a(3)	9.5640	9.4375	5.3996	3.4008	3.7432	7.7835	0.6078
					(−76)	(−32)	(−98)
Optimization problem (b)							
Case: b(1)	30.1743	31.5209	27.7745	29.9766	18.8039	0.5212	47.9376
					(23)	(−95)	(30)
Case: b(2)	**7.7790**	**9.5746**	**6.1873**	**4.5747**	**3.4413**	**4.0489**	**4.2403**
					(−76)	**(−65)**	**(−88)**
Case: b(3)	10.1112	9.9867	6.5318	4.8559	3.9536	6.6909	4.1755
					(−74)	(−42)	(−89)

The value in parenthesis denotes round-off percent increment over the corresponding value of the original mechanism.

Table 8
Parameters of the normalized original scraping machine mechanism

Link i	1	2	3	4	5	6	7
Link length, a_{ik}	1	3.02	3.02	8.78	6.27	6.27	6.27
Link mass, m_i^o	1	7.100	1.900	5.200	4.300	14.200	4.300
Centre of mass location, d_i^o	0.15	2.86	1.25	4.50	3.14	10.00	3.14
Centre of mass location, θ_i^o (°)	0	0	0	0	0	0	0
Moment of inertia, $\bar{I}_i^o$	0.4023	84.4028	5.8299	143.6004	61.5979	2007.2	61.5979

$O_1O_3 = 0.089$ m @ 180°; $O_1O_4 = 0.410$ m @ 84.7°; and $a_{12} = 0.038$ m; $m_1^o = 0.3260$ kg; $\omega_1 = 1$ rad/s.

are assigned arbitrarily as an equimomental conditions. Hence, the 28-dimensional design vector, $\mathbf{x}$, take form, according Eq. (45), as

$$\mathbf{x} \equiv [m_{11}, m_{12}, m_{13}, l_{11}, \cdots, m_{71}, m_{72}, m_{73}, l_{71}]^T.$$

Constraining link masses, m_i, between m_i^o and $5m_i^o$, and the variable l_{i1} between $0.5l_{i1}^o$ and $1.5l_{i1}^o$, the optimization problem for the scraping machine mechanism is posed as

$$\text{Minimize} \quad z = w_1\tilde{f}_{sh} + w_2\tilde{n}_{sh} \tag{53a}$$

$$\text{Subject to } m_i^o \leqslant (m_{i1} + m_{i2} + m_{i3}) \leqslant 5m_i^o \tag{53b}$$

$$0.5l_i^o \leqslant l_{i1} \leqslant 1.5l_i^o; \text{ for } i = 1, \ldots, 7. \tag{53c}$$

The shaking force and shaking moment are normalized with respect to parameters of the first link. Moreover, the point masses are allowed to take negative values. The whole algorithm is coded in the MATLAB environment to determine the time-dependent behaviour of the various relevant quantities, including the maximum bearing forces and driving torque.

The results obtained by applying different weighting factors, w_1 and w_2, are given in Table 9. These weighting factors are nothing but the importance given to different competing quantities. The values depend on the application and generally can be considered equal to each other. Three cases are investigated using three sets of the weighting factors, i.e., $(w_1, w_2) = (1.0, 0.0)$; $(0.5, 0.5)$; and $(0.0, 1.0)$. Fig. 10 shows a comparison to the dynamic performances of the mechanism. The RMS values of the dynamic quantities are compared with those corresponding values of the original mechanism in Table 10. The results show a significant improvement in the dynamic performances compared with those of the original one. For example, a reduction of 79%, 82%, and 98% is observed in the RMS values of input-torque, shaking force and shaking moment, respectively in case (2). The optimized total mass, its location, and moment of inertia of each link can be calculated from optimized point-masses using Eqs. (19)–(22).

Table 9
Design vector of the balanced scraping machine mechanism

Case: (w_1, w_2)	Design vector, $\mathbf{x}$
Case (1): (1.0, 0.0)	[−9.0271 3.1794 6.8477 0.6480 3.0299 3.1281 1.7513 1.9080 −0.8209 13.2130 −9.5284 2.6033 −8.4529 6.9753 6.6780 4.7979 0.1514 1.0659 3.0828 3.5648 2.3972 6.9384 6.8620 8.0674 17.7147 −5.6340 −5.7872 5.5376]^T
Case (2): (0.5, 0.5)	[−5.3548 −22.4369 28.7917 0.3592 −6.9162 4.9914 9.0249 1.7240 −70.8281 37.1001 43.2280 1.3079 22.0392 −6.4234 33.6626 2.8325 1.0194 −10.6993 13.9800 1.9142 7.8013 9.6599 −3.2613 5.9602 25.2464 −40.4415 19.4951 2.0326]^T
Case (3): (0.0, 1.0)	[0.4910 0.2545 0.2545 0.6343 −8.9417 21.7354 −5.1980 1.7240 −37.5079 14.1236 29.2331 0.8922 0.2026 −4.1376 21.8940 2.7065 4.9895 4.6985 −5.3880 5.6265 8.2713 9.8027 −3.8741 6.4858 26.5309 −19.9802 −2.2506 2.9904]^T

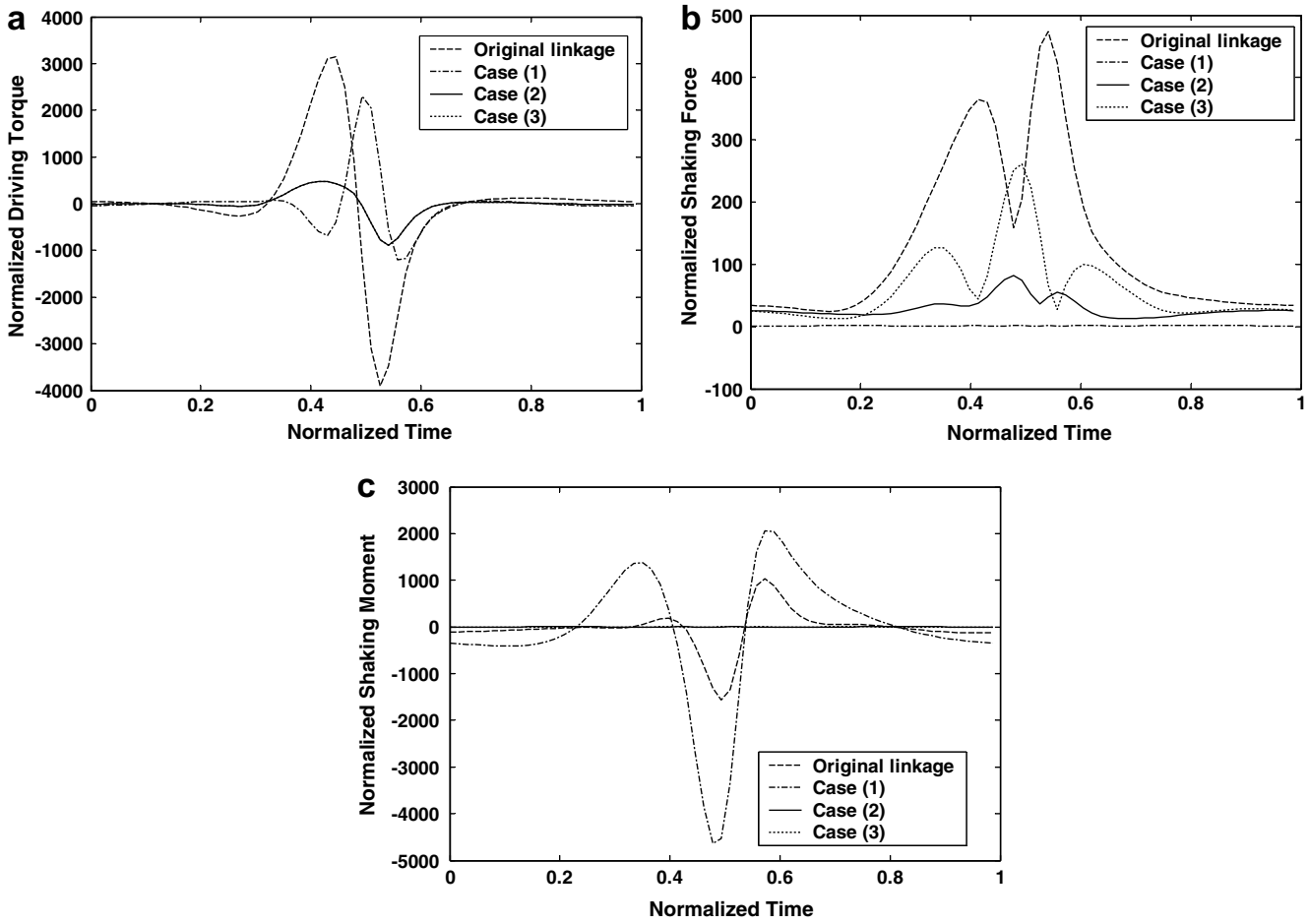

Fig. 10. Dynamic performance of the carpet scraping machine mechanism: (a) normalized driving torque, (b) normalized shaking force, (c) normalized shaking moment to fixed point O_1.

Table 10
Comparison of the RMS values of dynamic quantities between the original and the balanced scraping machine mechanism

Case	Input-torque, $\tilde{\tau}$	Shaking force, $\tilde{f}_{sh}$	Shaking moment, $\tilde{n}_{sh}$
Original	1192.30	182.40	413.50
Case: (1)	533.63	1.36	1337.60
$w_1 = 1.0$; $w_2 = 0.0$	(−55)	(−99)	(223)
Case: (2)	**245.02**	**32.74**	**5.32**
$\boldsymbol{w_1 = 0.5}$; $\boldsymbol{w_2 = 0.5}$	(**−79**)	(**−82**)	(**−98**)
Case: (3)	474.63	84.70	3.38
$w_1 = 0.0$; $w_2 = 1.0$	(−60)	(−54)	(−99)

The value in parenthesis denotes round-off percent increment over the corresponding value of the original mechanism.

5. Conclusions

This paper presents a generic formulation for the optimization of shaking force and shaking moment of single and multiloop planar mechanisms. The idea of equimomental system for a rigid body undergoing in a plane motion using three point-masses is introduced. Salient features of the point-mass model are highlighted there. The dynamic equations of motion for a link of the planar mechanism are formulated systematically in the parameters related to the equimomental point-masses. The constrained equations of motion in

minimal number are obtained in the relative joint coordinates. Dimension of equations is reduced to the number of independent generalized coordinates of the open system obtained by the cut-joint approach. The formulation leads to an optimization scheme for the mass distribution so that the dynamic performances, say, shaking force and moment, driving torque fluctuations, and the bearing reactions are minimized. The validation of the proposed method is done by comparing the analytical results available for the force balancing. The methodology is extended to the multiloop mechanism used in the carpet scraping machine. Total mass of the mechanism remain minimum or increase very little when the equimomental point mass are allowed to take negative. Trading off between the shaking force and shaking moment combine with equal weight to them shows optimum balancing. A significant improvement over the original mechanism in all the dynamic performances is obtained.

Appendix A. Derivation of equations of motion of a rigid body moving a plane

A set of three equimomental point-masses rigidly fixed in local frame OXY represents a rigid body, shown by the broken closed curve, Fig. 11. The points are moving in the XY plane, where OXY is the fixed inertial frame. Since the rigid body is represented as point masses, the equations of motion consist of only the Newton's equations motion. For the three point masses, there are six-dof. However, the distances between them are constants leading to three independent constraints. Hence, the effective dof is three. As a result, the system can be represented by three independent generalized coordinates, namely, two components of position vector $\mathbf{r}$ of the origin point O, and orientation $\boldsymbol{\alpha}$. Now, the equations of motion are derived in these minimal generalized coordinates. First, the Newton equations of the three points are given by

$$m_i\ddot{x}_i = f_{ix}; \quad m_i\ddot{y}_i = f_{iy} \quad \text{for } i = 1,2,3. \tag{A.1)–(A.2}$$

The Cartesian coordinates in the global frame of each point mass are obtained form Fig. 11 as

$$x_i = r_x + l_i\cos(\theta_i + \alpha); \quad y_i = r_y + l_i\sin(\theta_i + \alpha) \tag{A.3)–(A.4}$$

Differentiating Eqs. (A.3) and (A.4) twice w.r.t. time, one obtains

$$\dot{x}_i = \dot{r}_x - l_i\sin(\theta_i + \alpha)\dot{\alpha}; \quad \dot{y}_i = \dot{r}_x + l_i\cos(\theta_i + \alpha)\dot{\alpha} \tag{A.5)–(A.6}$$

and

$$\ddot{x}_i = \ddot{r}_x - l_i\cos(\theta_i + \alpha)\dot{\alpha}^2 - l_i\sin(\theta_i + \alpha)\ddot{\alpha} \tag{A.7}$$

$$\ddot{y}_i = \ddot{r}_x - l_i\sin(\theta_i + \alpha)\dot{\alpha}^2 + l_i\cos(\theta_i + \alpha)\ddot{\alpha} \tag{A.8}$$

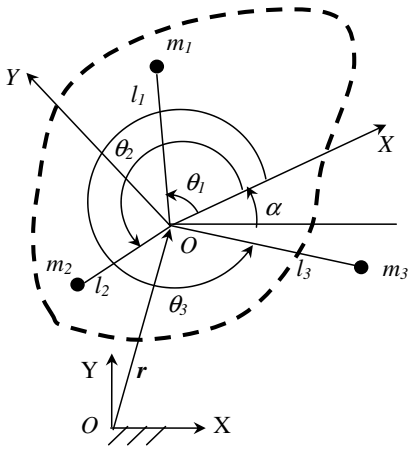

Fig. 11. A set of three point masses.

Using Eqs. (A.4) and (A.5), the generalized twist of the system of three points is given by

$$\mathbf{t} = \mathbf{N}\dot{\mathbf{q}} \tag{A.9}$$

where $\mathbf{t} \equiv [\mathbf{t}_1^{\mathrm{T}}, \cdots, \mathbf{t}_3^{\mathrm{T}}]^{\mathrm{T}}$ in which $\mathbf{t}_i \equiv [\dot{x}_i, \dot{y}_i]^{\mathrm{T}}$ and $\dot{\mathbf{q}} \equiv [\dot{\alpha}, \dot{r}_x, \dot{r}_y]^{\mathrm{T}}$. The 6×3 matrix, $\mathbf{N}$, is as follows:

$$\mathbf{N} \equiv \begin{bmatrix} -l_1 \sin(\theta_1 + \alpha) & 1 & 0 \\ l_1 \cos(\theta_1 + \alpha) & 0 & 1 \\ -l_2 \sin(\theta_2 + \alpha) & 1 & 0 \\ l_2 \cos(\theta_2 + \alpha) & 0 & 1 \\ -l_3 \sin(\theta_3 + \alpha) & 1 & 0 \\ l_1 \cos(\theta_3 + \alpha) & 0 & 1 \end{bmatrix} \tag{A.10}$$

The Newton equations of motion, Eqs. (A.1) and (A.2), for a point mass are now represented as

$$\mathbf{M}_i \dot{\mathbf{t}}_i = \mathbf{w}_i \tag{A.11}$$

where the 2×2 matrix, $\mathbf{M}_i$, and 2-vector of wrench, $\mathbf{w}_i$, are defined by $\mathbf{M}_i \equiv \begin{bmatrix} m_i & 0 \\ 0 & m_i \end{bmatrix} \mathbf{w}_i \equiv \begin{bmatrix} f_{ix} \\ f_{iy} \end{bmatrix}$. The twist rate, $\dot{\mathbf{t}}_i$, can be obtained from Eqs. (A.7) and (A.8) as

$$\dot{\mathbf{t}}_i \equiv \begin{bmatrix} \ddot{x}_i \\ \ddot{y}_i \end{bmatrix} = \begin{bmatrix} \ddot{r}_x - l_i \cos(\theta_i + \alpha)\dot{\alpha}^2 - l_i \sin(\theta_i + \alpha)\ddot{\alpha} \\ \ddot{r}_x - l_i \sin(\theta_i + \alpha)\dot{\alpha}^2 + l_i \cos(\theta_i + \alpha)\ddot{\alpha} \end{bmatrix} \tag{A.12}$$

Next the equations of motion for the three point masses are expressed together as

$$\mathbf{M}\dot{\mathbf{t}} = \mathbf{w} \tag{A.13}$$

where the 6×6 generalized mass matrix, $\mathbf{M} \equiv \mathrm{diag}[\mathbf{M}_1, \ldots, \mathbf{M}_3]$, and the 6-vector of generalized wrench, $\mathbf{w} \equiv [\mathbf{w}_1^{\mathrm{T}}, \cdots, \mathbf{w}_3^{\mathrm{T}}]^{\mathrm{T}}$. Pre-multiplying the transpose of the natural orthogonal complement, $\mathbf{N}$, to Eq. (A.10) gives the minimal constrained equations of motion, namely,

$$\mathbf{N}^{\mathrm{T}}\mathbf{M}\dot{\mathbf{t}} = \mathbf{N}^{\mathrm{T}}\mathbf{w} \tag{A.14}$$

On substitution of the transpose of $\mathbf{N}$ from Eq. (A.10), the equations of motion are obtained as

$$\begin{bmatrix} \sum_i m_i l_i^2 & -\sum_i m_i l_i \sin(\theta_i + \alpha) & \sum_i m_i l_i \cos(\theta_i + \alpha) \\ -\sum_i m_i l_i \cos(\theta_i + \alpha) & \sum_i m_i & 0 \\ \sum_i m_i l_i \sin(\theta_i + \alpha) & 0 & \sum_i m_i \end{bmatrix} \begin{bmatrix} \ddot{\alpha} \\ \ddot{r}_x \\ \ddot{r}_y \end{bmatrix} + \begin{bmatrix} 0 & 0 & 0 \\ \sum_i m_i l_i \cos(\theta_i + \alpha) & 0 & 0 \\ \sum_i m_i l_i \sin(\theta_i + \alpha) & 0 & 0 \end{bmatrix} \begin{bmatrix} \dot{\alpha} \\ \dot{r}_x \\ \dot{r}_y \end{bmatrix} = \begin{bmatrix} -\sum_i m_i l_i f_{ix} \sin(\theta_i + \alpha) + \sum_i m_i l_i f_{iy} \cos(\theta_i + \alpha) \\ \sum_i f_{ix} \\ \sum_i f_{iy} \end{bmatrix} \tag{A.15}$$

In Eq. (A.15), the right-hand side is the generalized forces along the three generalized coordinates, r_x, r_y, α. The 3-vectors, $[\dot{\alpha}, \dot{r}_x, \dot{r}_y]^{\mathrm{T}}$ and $[\ddot{\alpha}, \ddot{r}_x, \ddot{r}_y]^{\mathrm{T}}$, are the first and second time derivatives of generalized coordinates, respectively.

Appendix B. Comparison between two and three point-mass models

The dynamically equivalent system, called here as an equimomental system, of point-masses of a rigid link moving in a plane requires at least two point-masses. The representation of each link by equimomental system of two point-masses is referred as two point-mass model. Similarly, equimomental system of three point-masses is called three point-mass model, and so on. Balancing of a mechanism using the three point-mass

model is shown in Section 3, whereas two point-mass model is discussed in [28]. Note that each mass requires three parameters, m_{ij}, l_{ij}, and θ_{ij} to identify it, a total of 6 and 9 parameters are necessary to completely define the equimomental system of 2 and 3 point-mass models, respectively. Representation of rigid link as a dynamically equivalent system of point-masses, the point-mass parameters must satisfy the equimomental conditions, Eqs. (1)–(4). The determination of these parameters is discussed in Section 2. Comparison of these models is given in Table 11 and illustrated in Fig. 12.

To show effectiveness of the three point-mass model in comparison with that of the two point-mass model in the balancing of mechanisms, the optimization problem is reformulated here using both the models. The shaking force and shaking moment are computed using the same dynamic algorithm, as explained in Sections 3.1 and 3.2. Note that the matrices, $\mathbf{M}_i$ and $\mathbf{C}_i$, are modified corresponding to the model chosen for the representation of a rigid link.

Eqs. (23)–(26) are the equations of motion for the ith link in terms of its $3p$ point-mass parameters, namely, $m_{ij}, \theta_{ij}, l_{ij}$, for $j = 1, \ldots, p$, where $p = 2$ and 3 for two and three point-mass models, respectively. Now, all or some of the point-mass parameters can be used as design variables based on their influence on the objective function of an optimization problem. For example, as evident from Eq. (22), the angles, θ_{ij}, do not influence the moment of inertia, however, the distances, l_{ij}, do. Hence, the angles, θ_{ij}, are excluded from the set of design variables. In some research papers, namely, by Wiederrich and Roth [17], Lee and Cheng [23], and Chaudhary and Saha [28], two point-mass model was considered to represent the mass and inertia of a link. They assumed, $\theta_{i1} = 0$ and $\theta_{i2} = \pi/2$, amongst the six parameters m_{i1}, m_{i2}, θ_{i1}, θ_{i2}, l_{i1}, and l_{i2}. The remaining parameters were then considered as design variables. In this paper, instead, three-point mass model is proposed.

To compare the both models it is required that the design variables and constraints on them are considered in same manner. The design variables for the two point-mass model are m_{ij} and l_{ij} for $j = 1, 2$, where $\theta_{i1} = 0$ and $\theta_{i2} = \pi/2$ [28]. Similarly, for the three point-mass model, one may choose two parameters per link, i.e., m_{ij} and l_{ij} for $j = 1, 2, 3$, as design variables, and $\theta_{i1} = 0$; $\theta_{i2} = 2\pi/3$; and $\theta_{i3} = 4\pi/3$ to place the masses symmetrically. Note here that the number of design variables can be further reduced for the optimization. The four parameters for each link, namely, m_{i1}, m_{i2}, m_{i3}, and l_{i1}, are treated in this paper as design variables.

Using the same constraint bounds on the mass and the inertia of the links, the optimization problems can be posed as

$$\text{Minimize } z(x) = w_1 \tilde{f}_{\text{sh}} + w_2 \tilde{n}_{\text{sh}} \tag{B.1}$$

Table 11
Comparison between two and three point-mass models

Criterion	Two point-mass	Three point-mass
Point-mass parameters	6: Parameters per link m_{ij}, θ_{ij}, l_{ij}, for $j = 1, 2$	9: Parameters per link m_{ij}, θ_{ij}, l_{ij}, for $j = 1, 2, 3$
Determination of the parameters for given link	Assume any two and compute remaining four	Assume any five and compute remaining four
Suitable choice for assumptions	$\theta_{i1} = 0$ and $\theta_{i2} = \pi/2$ [23]	$\theta_{i1} = 0$;$\theta_{i2} = 2\pi/3$; $\theta_{i3} = 4\pi/3$; and $l_{i2} = l_{i3} = l_{i1}$

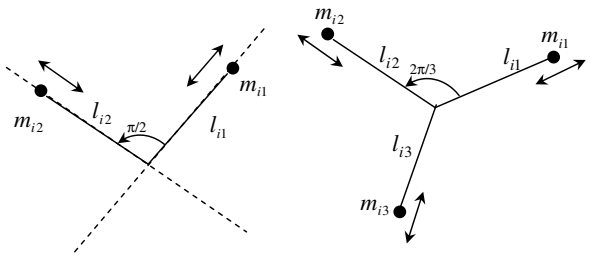

Fig. 12. Two and three point-mass models.

Table 12
Comparison of performance

Balancing method	Number of iteration	RMS values		
		Driving torque	Shaking force	Shaking moment[a]
Example 1: Hoeken's four-bar mechanism				
Original linkage	–	15.32	11.54	36.78
Two point-mass model:	55	1.24	5.67	4.34
$w_1 = 0.5$; $w_2 = 0.5$		(−92)[b]	(−51)	(−88)
Three point-mass model:	40	2.15	0.05	3.44
$w_1 = 0.5$; $w_2 = 0.5$		(−86)	(−100)	(−91)
Example 2: Carpet scraping machine mechanism				
Original linkage		1192.30	182.40	413.50
Two point-mass model:	93	519.37	55.19	14.50
$w_1 = 0.5$; $w_2 = 0.5$		(−56)	(−70)	(−96)
Three point-mass model:	93	230.47	51.14	25.30
$w_1 = 0.5$; $w_2 = 0.5$		(−81)	(−72)	(−94)

[a] The shaking moment is taken with respect to the driving joint.
[b] The values in the parentheses denote the percentage increment/decrement over the corresponding RMS values of the original linkage.

For two point-mass model

$$\text{Subject to } m_i^{\mathrm{o}} \leqslant (m_{i1} + m_{i2}) \leqslant 5m_i^{\mathrm{o}} \tag{B.2}$$

$$0.25I_i^{\mathrm{o}} \leqslant (m_{i1}l_{i1}^2 + m_{i2}l_{i2}^2) \tag{B.3}$$

For three point-mass model

$$\text{Subject to } m_i^{\mathrm{o}} \leqslant (m_{i1} + m_{i2} + m_{i3}) \leqslant 5m_i^{\mathrm{o}} \tag{B.4}$$

$$0.25I_i^{\mathrm{o}} \leqslant (m_{i1}l_{i1}^2 + m_{i2}l_{i2}^2 + m_{i3}l_{i3}^2) \tag{B.5}$$

Examples 1 and 2 given in Section 4 are considered for analysis purpose. The optimization problem posed in Eqs. (B.1)–(B.5) is solved using MATLAB optimization toolbox under the same tolerances for the termination of the functions and the design variables. The RMS values of the dynamic quantities obtained using both the models are compared in Table 12. With more number of point-masses, the optimization algorithm quickly redistributes the link masses with better performances in both the examples. Hence, it is concluded that three point-mass model is better to balance planar mechanisms. The analytical proof is beyond the scope of this paper, and will be taken up as future studies.

References

[1] V.A. Shchepetilńikov, The determination of the mass centres of mechanisms in connection with the problem of mechanism balancing, Journal of Mechanism 3 (1968) 367–389.
[2] R.S. Berkof, G.G. Lowen, A new method for completely force balancing simple linkages, Transactions of ASME, Journal of Engineering for Industry 91 (1) (1969) 21–26.
[3] I.S. Kosav, A new general method for full force balancing of planar linkages, Mechanism and Machine Theory 23 (6) (1988) 475–480.
[4] G.G. Lowen, F.R. Tepper, R.S. Berkof, The quantitative influence of complete force balancing on the forces and moments of certain families of four-bar linkages, Mechanism and Machine Theory 9 (1974) 299–323.
[5] J.L. Elliott, D. Tesar, The theory of torque, shaking force, and shaking moment balancing of four link mechanisms, Transactions of ASME, Journal of Engineering for Industry 99 (3) (1977) 715–722.
[6] V.A. Kamenskii, On the questions of the balancing of plane linkages, Journal of Mechanism 3 (1968) 303–322.
[7] R.S. Berkof, Complete force and moment balancing of inline four-bar linkage, Mechanism and Machine Theory 8 (1973) 397–410.
[8] I. Esat, H. Bahai, A theory of complete force and moment balancing of planar linkage mechanisms, Mechanism and Machine Theory 34 (1999) 903–922.
[9] Z. Ye, M.R. Smith, Complete balancing of planar linkages by an equivalent method, Mechanism and Machine Theory 29 (5) (1994) 701–712.
[10] V.H. Arakelian, M.R. Smith, Complete shaking force and shaking moment balancing of linkages, Mechanism and Machine Theory 34 (1999) 1141–1153.

[11] I.S. Koshav, General theory of complete shaking moment balancing of planar linkages: a critical review, Mechanism and Machine Theory 35 (2000) 1501–1514.
[12] V.H. Arakelian, M.R. Smith, Shaking force and shaking moment balancing of mechanisms: a historical review with new examples, Transactions of ASME Journal of Mechanical Design 127 (2005) 334–339.
[13] R.S. Berkof, G.G. Lowen, Theory of shaking moment optimization of forced-balanced four-bar linkages, Transactions of ASME Journal of Engineering for Industry 93B (1) (1971) 53–60.
[14] W.L. Carson, J.M. Stephenes, Feasible parameter design spaces for force and root-mean-square moment balancing an in-line 4R 4-bar synthesized for kinematic criteria, Mechanism and Machine Theory 13 (1978) 649–658.
[15] R.S. Hains, Minimum RMS shaking moment or driving torque of a force-balanced linkage using feasible counterweights, Mechanism and Machine Theory 16 (1981) 185–190.
[16] V. Arakelian, M. Dahan, Partial shaking moment balancing of fully force balanced linkages, Mechanism and Machine Theory 36 (2001) 1241–1252.
[17] J. L Wiederrich, B. Roth, Momentum balancing of four-bar linkages, Transactions of ASME Journal of Engineering for Industry 98 (4) (1976) 1285–1289.
[18] E. J Routh, Treatise on the Dynamics of a System of Rigid Bodies, Elementary Part I, Dover Publication Inc., New York, 1905.
[19] R.A. Wenglarz, A.A. Forarasy, L. Maunder, Simplified dynamic models, Engineering 208 (1969) 194–195.
[20] N.C. Huang, Equimomental system of rigidly connected equal particles, Journal of Guidance, Control and Dynamics 16 (6) (1983) 1194–1196.
[21] A.A. Sherwood, B.A. Hockey, The optimization of mass distribution in mechanisms using dynamically similar systems, Journal of Mechanism 4 (1969) 243–260.
[22] B.A. Hockey, The minimization of the fluctuation of input-shaft torque in plane mechanisms, Mechanism and Machine Theory 7 (1972) 335–346.
[23] T.W. Lee, C. Cheng, Optimum balancing of combined shaking force, shaking moment, and torque fluctuations in high speed linkages, Transactions of ASME Journal of Mechanisms, Transmissions, and Automation in Design 106 (2) (1984) 242–251.
[24] S. Molian, Kinematics and dynamics of the RSSR mechanism, Mechanism and Machine Theory 8 (1973) 271–282.
[25] H.A. Attia, A matrix formulation for the dynamic analysis of spatial mechanisms using point coordinates and velocity transformation, Acta Mechanica 165 (2003) 207–222.
[26] G.S. Gill, F. Freudenstein, Minimization of inertia-induced forces in spherical four-bar mechanisms. Part 1: the general spherical four-bar linkage, Transactions of ASME Journal of Mechanisms, Transmissions, and Automation in Design 105 (1983) 471–477.
[27] S. Rahman, Reduction of inertia-induced forces in a generalized spatial mechanism, Ph.D. Thesis, Dept. of Mech. Eng., The New Jersey Institute of Technology, <http://www.library.njit.edu/etd/1990s/1996/njit-etd1996-017/njit-etd1996-017.html>.
[28] H. Chaudhary, S.K. Saha, Balancing of four-bar linkages using maximum recursive dynamic algorithm, Mechanism and Machine Theory 42 (2) (2007) 216–232.
[29] P.E. Nikravesh, Systematic reduction of multibody equations of motion to a minimal set, International Journal of Non-Linear Mechanics 25 (2/3) (1990) 143–151.
[30] J. Angeles, S. Lee, The formulation of dynamical equations of holonomic mechanical systems using a natural orthogonal complement, Transactions of ASME, Journal of Applied Mechanics 55 (1988) 243–244.
[31] S.K. Saha, Dynamics of serial multibody systems using the decoupled natural orthogonal complement matrices, Transactions of ASME, Journal of Applied Mechanics 66 (4) (1999) 986–996.
[32] S.K. Saha, R. Prasad, A.K. Mandal, Use of Hoeken's and Pantograph mechanisms for carpet scraping operations, in: S.K. Saha (Ed.), Proceedings of 11th National Conference On Machines and Mechanisms, Allied Publishers Pvt. Limited, New Delhi, 2003, pp. 732–738.
[33] A.A. Shabana, Computational Dynamics, Wiley, New York, 1994.
[34] MATLAB, 2004, Optimization Toolbox, Version 7.0.0.19920 (R14).
[35] F.L. Conte, G.R. George, R.W. Mayne, J.P. Sadler, Optimum mechanism design combining kinematic and dynamic-force considerations, Transactions of ASME Journal of Engineering for Industry 95 (2) (1975) 662–670.